AD-A115 403 STANFORD UNIV CA STANFORD ELECTRONICS LABS F/G 7/4
STUDY OF THE ELECTRONIC SURFACE STATES OF III-V COMPOUNDS AND S--ETC(U)
MAR 81 W E SPICER, I LINDAU N00014-79-C-0072
UNCLASSIFIED NL

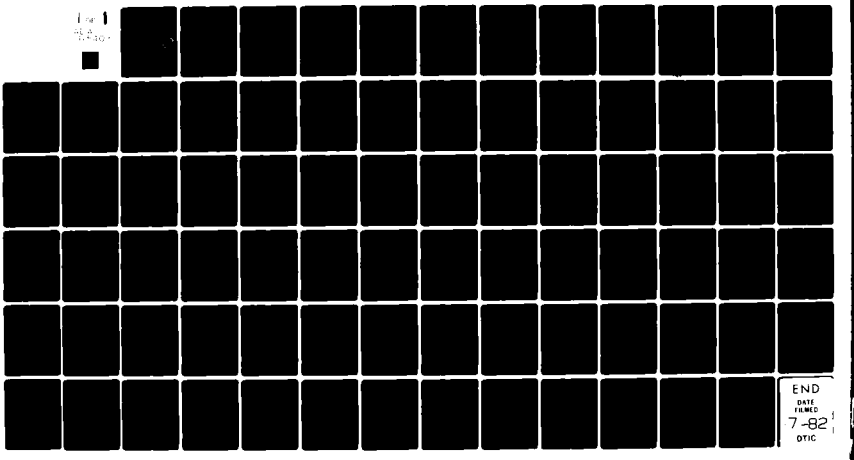

END
DATE FILMED
7-82
DTIC

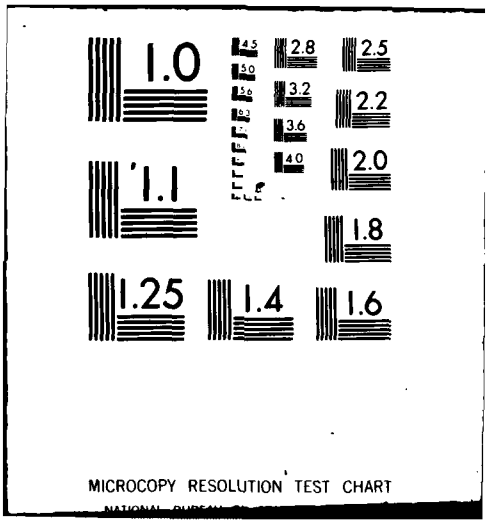
1.0
1.1
1.25
1.4
1.6
1.8
2.0
2.2
2.5
2.8
3.2
3.6
4.0
4.5
5.0
5.6
6.3
MICROCOPY RESOLUTION TEST CHART

(12)

SOLID STATE ELECTRONICS LABORATORY

STANFORD ELECTRONICS LABORATORIES
DEPARTMENT OF ELECTRICAL ENGINEERING
STANFORD UNIVERSITY · STANFORD, CA 94305

STUDY OF THE ELECTRONIC SURFACE STATES OF III-V COMPOUNDS AND SILICON

Semi-Annual Technical Progress Report

1 October 1980 to 31 March 1981

Principal Investigators:

W. E. Spicer
I. Lindau

Telephone: (415) 497-4643

Office of Naval Research
Department of the Navy
Arlington, Virginia 22217

Sponsored by

DEFENSE ADVANCED RESEARCH PROJECTS AGENCY
DARPA Order No. 3564
Program Code No. HX1241

Contract No. N00014-79-C-0072

Effective: 1 October 1980 Expiration: 30 September 1981 (237,629)

Stanford Electronics Laboratories
Stanford University
Stanford, California 94305

The views and conclusions contained in this document are those of the authors and should not be interpreted as necessarily representing the official policies, either expressed or implied, of the Defense Advanced Research Projects Agency or the U.S. Government.

(12)

STUDY OF THE ELECTRONIC SURFACE STATES OF III-V COMPOUNDS AND SILICON

Semi-Annual Technical Progress Report

1 October 1980 to 31 March 1981

Principal Investigators:

W. E. Spicer
I. Lindau

Telephone: (415) 497-4643

Office of Naval Research
Department of the Navy
Arlington, Virginia 22217

Sponsored by

DEFENSE ADVANCED RESEARCH PROJECTS AGENCY
DARPA Order No. 3564
Program Code No. HX1241

Contract No. N00014-79-C-0072

Effective: 1 October 1980 Expiration: 30 September 1981 ($237,629)

Stanford Electronics Laboratories
Stanford University
Stanford, California 94305

CONTENTS

Chapter I

OVERVIEW

Our work has continued to progress in several areas. We list here the topics that comprise the majority of our efforts.

1. Si-Metal Contacts: We have investigated a number of transition metals (Ni, Pd, Pt, Ag) on Si to determine both the abruptness of the interface and the nature of the chemical bonding between Si and the metal. We have also examined in some detail the removal of the surface states on a cleaved Si surface by oxygen, cesium, and transition metals. These studies have advanced our understanding of the mechanism of Schottky barrier formation on Si.

2. Laser Enhanced Oxidation of GaAs (110): We have demonstrated an increase in the oxygen sticking probability on the GaAs (110) surface by exposure to low-intensity ($\lesssim 3 w/cm^2$) laser radiation. We believe this enhancement is due to an increase in the density of free electrons at or near the surface.

3. Oxygen Chemisorption on GaAs (110): New valence band measurements, sensitive to very low (<0.001 monolayer) oxygen on GaAs (110) consists of an oxygen bonded to a surface As in addition to an oxygen bridging between that As and a next nearest Ga.

4. Interface Between GaAs-Cs, O, and Vacuum in NEA Photocathodes: We have completed work which gives fundamental insight into the GaAs-Cs-O interface region and opens new possibilities for reducing the threshold of response (by using 3-5 semiconductor alloys) of negative electron affinity photocathodes, as well as making stable cathodes at lower wavelengths.

5. Interaction of Oxygen with Si (111): We have investigated the oxygen adsorption properties on both the Si surface cleaved at room temperature (which exhibits a 2 x 1 reconstruction) and the annealed surface (7 x 7 reconstruction). Our results have shown unambiguous support for the defect type model of the 7 x 7 surface.

6. Adsorption of Column III and V Elements on GaAs: We have found that the column III elements studied (Ga and Al) appear to form a metallic bond to the surface, thus forming two-dimensional "rafts" randomly oriented on the GaAs surface. In contrast, the column V element (Sb) gives evidence of a directional bond, resulting in an ordered overlayer.

Chapter II

SUMMARY OF SELECTED TOPICS

Brief summaries of the aforementioned topics (1) and (4) are included here; summaries of the other topics will be found in the previous and upcoming reports of this contract year. More detailed accounts of our work in these areas appear in the appendices of this report, as well as the appendices of previous and upcoming reports. Further information will be found in our proposal for the renewal of Contract No. N00014-79-C-0072 for the period 1 October 1981 to 30 September 1982.

A. Si-Metal Contacts

One area of extreme importance is to understand on a microscopic scale the Si/transition metal interface regarding: (a) the abruptness of the interface; (b) the nature of the chemical bonding between Si and the transition metal; and (c) the effect of oxide layers and other impurities. We have made considerable progress on the problems listed under (a) and (b).

We have, in particular, studied the Pd/Si (111) interface in great detail from metal coverages of 0.5 to 23 monolayers. We enclose as Appendix E a reprint of a paper presented at the PCSI-8 conference and published in J. Vac. Sci. Tech. Of particular importance is that a nearly stoichiometric Pd_2Si compound is formed at room temperature at monolayer coverages (elevated temperatures are required to form the bulk silicide). However, a close examination of the interface on a microscopic scale reveals that there is a concentration gradient across the interface and the Si/Pd_2Si interface is not atomically abrupt. This problem has been addressed earlier by ourselves and a number of other groups, but it is just during the last year that we have achieved a more detailed understanding of the Pd/Si (111)

interface on a microscopic scale (Appendix E). Our recent work shows that the graded interface extends for several atomic layers between Si and Pd_2Si. The abruptness of the interface is comparable to that for Pt/Si (111) but is less pronounced than for the Ni/Si (111) and Cu/Si (111) interfaces (and, of course, the Ag/Si (111) interface--see below).

We have also established a detailed understanding of the chemical bonding between Pd and the Si substrate (see Appendic C, which is a reprint of a paper published in Solid State Comm.). By exploiting the Cooper minimum technique (which we have developed), we have been able to determine the orbital character (s, p, or d) of the electronic levels involved in the interface bonding. The photoemission spectra of the valence band have characteristic features which can be identified with the breaking of the tetrahedral coordination in Si. This has been used as a marker to follow the interaction between Pd and Si. Further detailed changes in the valence band show how the bonding is changing and evolving across the interface from the Si substrate via the Pd/Si intermixed region to the Pd_2Si bulk compound. It is noteworthy that the Pd 4d band, which intersects the Fermi level with a high density of states in the pure metal, is pulled down about 2 eV below the Fermi level in Pd/Si, rendering a noble metal resemblance to the spectra. However, the Si 2p core level spectra show that the charge transfer between Si and Pd is very small and the observed change can thus not be explained as a simple charge transfer from Si to Pd, which would result in a filled 4d band. Instead, we now believe that Si acts as a very strong "scatterer" and changes the sp to d hybridization in the Pd metal.

Finally, we want to point out that Ag/Si (111) is by far the most abrupt interface we have studied so far. However, all existing models are based on epitaxial growth of Ag on Si without any Ag-Si interaction (bonding). Our

photoemission data clearly show that there is a fairly strong Ag-Si interaction leading to a breaking of the tetrahedral coordination in Si. The differences in the intermixed region in metal/Si interfaces is thus at most a quantitative, with increasing intermixing going from Ag/Si, Cu/Si, Ni/Si, PdSi to Au/Si. This observation may have some important implications for device fabrication. A thin metal layer (about one monolayer) of Ag followed by, for instance, Pd deposition may insure an extremely abrupt interface in addition to a stable Pd_2Si silicide.

B. Interface Between GaAs-Cs, O, and Vacuum in NEA Photocathodes

An important result of a DARPA program started approximately a decade ago is the GaAs negative affinity photocathode for third generation night vision goggles. These have been proven to be superior to the standard second generation goggles (S-20 cathodes), have undergone considerable field testing, and are now approaching a relatively large scale production phase.

These cathodes re unique in that they are the first (in 50 years) to have been scientifically engineered (to a large extent) rather than to have been developed almost entirely by empirical trial-and-error methods. In fact, the region between the GaAs and the vacuum which gives the negative electron affinity was not understood on anything approaching a basic level, although conflicting models had been proposed to explain it.

This year we have completed work which gives fundamental insight into the interface region and opens new possibilities for reducing the threshold of response (by using 3-5 semiconductor alloys) and making stable cathodes at lower wavelengths. In addition, and perhaps more importantly, it may lead to more efficient processing of the existing GaAs cathode. This could lead to increased yield (with cost reductions) and improved performance.

The first finding was that, with a monolayer of Cs coverage, the sticking coefficient of oxygen on GaAs (110) is increased by about a factor of 10^9 (a billion). Further, the oxygen does not combine chemically with the Cs but bonds first to the As (chemisorption) and then to the Ga of the GaAs. Not being sure whether this phenomenon took place in the activation of practical cathodes, we adopted the activation process used for practical cathodes and measured sensitivity in uA/lumen so that our results could be compared with the practical results. The earlier results were confirmed in this recent work.

The breakthrough lies in recognizing: (1) that a GaAs-oxygen layer lies between the surface oxygen-Cs layer (a possibility overlooked in all previous models); (2) that it is this layer which forms the harmful heterojunction barrier which lies between the GaAs and O-Cs; (3) that present processing technology does not consider the build-up of this layer (or try to minimize it); and (4) if (based on our new knowledge) alternate activation techniques could be developed, this harmful barrier might be reduced or minimized.

APPENDICES

A. C. Y. Su, P. R. Skeath, I. Lindau, and W. E. Spicer, "The Nature of the 7 x 7 Reconstruction of Si(111): As Revealed by Changes in Oxygen Sorption from 2 x 1 to 7 x 7," Surf. Sci. 107, L355 (1981).

B. Perry Skeath, C. Y. Su, I. Lindau, and W. E. Spicer, "Bonding of Column 3 and 5 Atoms on GaAs(110)," Solid St. Comm. 40, 873, (1981).

C. G. Rossi, I. Abbati, L. Braicovich, I. Lindau, and W. E. Spicer, "Nature of the Valence States in Silicon Transition Metal Interfaces," Solid St. Comm. 39, 195 (1981).

D. C. Y. Su, P. R. Skeath, I. Lindau, and W. E. Spicer, "Oxidation of Si(111), 7 x 7 and 2 x 1: A Comparison," J. Vac. Sci. Technol. 18, 843 (1981).

E. I. Abbati, G. Rossi, I. Lindau, and W. E. Spicer, "Exploiting Energy-dependent Photoemission in Si d-metal Interfaces: The Si(111)-Pd Case," J. Vac. Sci. Technol. 19, 636 (1981).

F. W. E. Spicer, P. Skeath, C. Y. Su, and I. Lindau, "Fermi Level Pinning at 3-5 Semiconductor Interfaces," Proc. 15th Int. Conf. Phys. Semic. (Kyoto, 1980), J. Phys. Soc. Japan 49 Suppl. A, 1079 (1980).

G. W. E. Spicer, I. Lindau, P. R. Skeath, and C. Y. Su, "A Unified Model for Schottky Barrier Formation and MOS Interface States on 3-5 Compounds," 3rd Symposium Appl. Surf. Anal. (1980), to be published in Appl. Surf. Sci.

H. Chung-Yi Su, I. Lindau, and W. E. Spicer, "Photoemission Studies of the Oxidation of Cs^+ -- Identification of the Multiplet Structures of Oxygen Species," submitted to Chem. Phys. Lett.

APPENDIX A

Surface Science 107 (1981) L355–L361
North-Holland Publishing Company

SURFACE SCIENCE LETTERS

THE NATURE OF THE 7 X 7 RECONSTRUCTION OF Si(111): AS REVEALED BY CHANGES IN OXYGEN SORPTION FROM 2 X 1 TO 7 X 7 *

C.Y. SU, P.R. SKEATH, I. LINDAU and W.E. SPICER **
Electrical Engineering Department, Stanford University, Stanford, California 94305, USA

Received 9 February 1981

Room temperature adsorption of oxygen on 2 x 1 and 7 x 7 reconstructed Si(111) surfaces is shown by core level shift and sticking coeffcients to proceed differently, indicating strongly different nature of the two reconstructions and supporting the defect type models for the 7 x 7 reconstruction.

We report experimental evidence showing clear difference between the oxygen adsorption properties of the 2 X 1 and 7 X 7 surfaces. The significance of this new finding is twofold: (i) it provides new information that strongly supports the "defect" type models for the 7 X 7 structure; (ii) it demonstrates the importance of surface reconstructions in affecting the oxygen adsorption processes, which has not been recognized in the past.

Cleaved Si(111) surface has a 2 X 1 reconstruction, it transforms to a 7 X 7 reconstruction when subsequently heated to ~400°C [1]. The nature of the 2 X 1 to 7 X 7 transformation is pivotal to understanding the critical problem of surface reconstructions of covalent semiconductors. The 2 X 1 reconstruction is generally accepted as rows of surface atoms being electronically driven to alternately raise and lower [2]. The 7 X 7 reconstruction, however, has been explained on the bases of two radically different classes of models. They represent fundamentally different ways a covalent semiconductor surface adjusting itself to reach the most stable structure when the necessary activation energy for transformation is supplied (by heating in this case). In one class of models, the surface is electronically driven to adjust within a small perturbation of a smooth plane (which is defined by the constraints of the bulk crystalline structure). We will call this "weak perturbation" class of models [3]. In the other class, the surface atoms migrate a significant number of lattice sites to create "defects" in a smooth surface. This class we will term

* Work supported by DARPA (Contract No. DAAK02-74-C0069).
** Stanford Asherman Professor of Engineering.

0039–6028/81/0000–0000/$ 02.50

as "defect" models [4]. To claim full knowledge of the bonding in covalent semiconductors, one should be able to choose between these two drastically different types of surface reconstructions. However, this old problem is still unresolved and quite alive, as exemplified by two recent Physical Review Letters each putting forward a specific model within an opposite class of models (Chadi et al. [5] and Phillips [6]).

Clearly, experimental input is critical to resolving this issue. Determination of the exact positions of atoms in the 7 × 7 structure through LEED techniques is not a feasible task because of the great complexity of this structure. In the mid-seventies, gas adsorption experiments involving hydrogen [7] and chlorine [8] have provided a simple test to distinguish the two types of reconstruction theory. There preservation of the 7 × 7 structure, as opposed to the destruction of the 2 × 1 structure, upon hydrogen [7] and chlorine [8] adsorption strongly supports the "defect" type models. Employing gas adsorption experiments to distinguish reconstruction models is a particularly viable approach here because the 2 × 1 structure can be taken as a "known reference" for the "weak perturbation" type surfaces in considering adsorption behavior. In the present case, we have adopted the same general approach with oxygen as the particular adsorbate. One advantage of the present study is that the oxygen induced Si core level shifts can very sensitively reveal differences in the final Si–O bonding complex, which, in turn, facilitate more definite comparison between the adsorption properties of the 2 × 1 and 7 × 7 surfaces. In early studies of hydrogenation or chlorination, differences or similarities between the final Si–H or Si–Cl bonding complex formed on the two surfaces were less well determined. Perhaps such uncertainty is the reason that, as can be seen from recent publications [5,6], H and Cl experiments did not settle the matter, thus making new experimental work imperative.

We have measured the valence spectra and the chemical shifts in Si-2p core level upon oxygen adsorption. High energy resolution (0.35 eV) and surface sensitivity were achieved in photoemission experiments by utilizing 130 eV synchrotron radiation from the Stanford Synchrotron Radiation Laboratory (SSRL). Oxygen exposures and photoemission measurements were performed in an ultra-high vacuum system with base pressure of $3 \sim 5 \times 10^{-11}$ Torr. 2 × 1 surfaces were prepared by cleaving in situ, and 7 × 7 surfaces were prepared by thermal conversion (>500°C for >20 min) of in situ cleaved surfaces. Sharp 7 × 7 LEED patterns were observed after such treatment. O-1s level was also measured with a Mg-Kα X-ray source.

Fig. 1 gives the valence band region spectra of a 7 × 7 surface exposed to 100 L oxygen (curve (a), i.e. 10^{-6} Torr for 100 s), and a 2 × 1 surface first exposed to 1000 L oxygen (curve (b), 10^{-6} Torr for 1000 s) and then annealed at 350°C for 10 min (curve (c)). The bottom curve is a spectrum of a clean surface, and is plotted here to illustrate that the peak at ~3.2 eV binding energy (BE) is due to substrate emission. The dominant feature due to oxygen adsorption is the peak at 6.8 eV BE. The relative height of the 6.8 eV peak to the 3.2 eV peak is thus a measure of the oxgyen coverage. It is seen that oxygen coverages are equal within

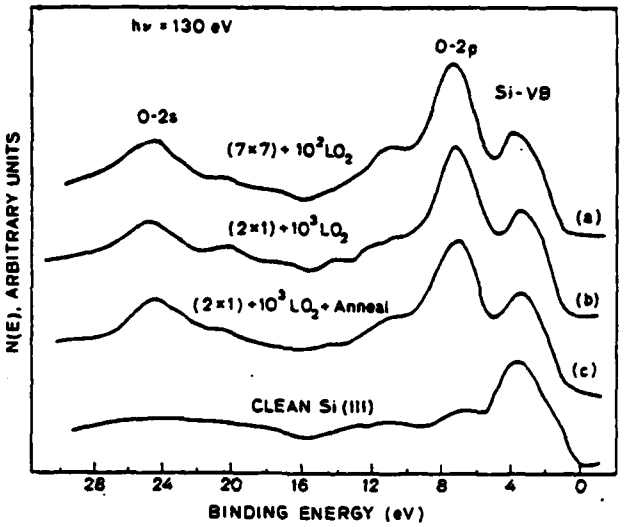

Fig. 1. The valence band region spectra of surfaces prepared in different ways: (a) a 7 × 7 surface exposed to 100 L O_2, (b) a 2 × 1 surface exposed to 1000 L O_2 and then annealed at 350°C for 10 min (c). The bottom curve is the spectrum of a clean surface.

experimental error (±10%) in all three cases shown. This point was also established by comparing O-1s intensities from each case. For 7 × 7 surfaces subjected to increasing oxygen exposure from 100 L to as high as 10^5 L, no increase in oxygen intensity was measured. Thus oxygen adsorption on the 7 × 7 surface reaches "saturation" [9] at or below 100 L. Long experience with our cleaved 2 × 1 surface has shown oxygen "saturation" to occur at 1000 L [10,11]. (Here "saturation" is not as sharp as for the 7 × 7, but is characterized by orders of magnitude drop in the rate of uptake.) Thus, the sticking coefficient is at least a factor of 10 higher on the 7 × 7 surface. The results of equal oxygen coverage on the 2 × 1 and 7 × 7 surfaces at "saturation" and the higher sticking coefficient on the 7 × 7 surface are consistent with earlier results [9,12,13], and favor the "defect" model to some extent. This is because the higher reactivity to oxygen of the 7 × 7 surface is not expected to be explained by a structure very similar to the 2 × 1 reconstruction. For all models in the defect class, we observe the presence of a significant number of unsatisfied bonds near "defect" sites, which can easily explain the higher reactivity.

Fig. 2 gives the Si-2p core level spectra of the corresponding surfaces of fig. 1. Here we see at once large difference. Fig. 1a shows Si-2p core level of a 7 × 7 surface before and after 100 L oxygen exposure. The broad oxygen-induced shift contains several components, with the largest chemical shift being ~3.4 eV, and thus indicates the existence of strongly inequivalent groups of surface atoms in the

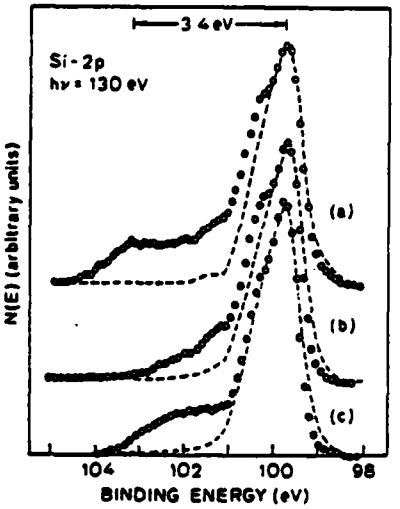

Fig. 2. Si-2p core level spectra of the corresponding surfaces in fig. 1. Dashed curves are Si-2p level spectra for clean surfaces.

clean 7 × 7 structure. In the models within the "defect class" we can easily identify such distinctly inequivalent groups, hence this finding is taken as strongly supporting the "defect" type model. This finding is against the "weak perturbation" model, because in a structure close to the smooth plane no such inequivalent groups of atoms can be unambiguously identified; in particular, we cannot identify a special group of Si atoms that can easily achieve, at room temperature, high oxygen coordination number, which is required by the presence of the 3.4 eV shift. The above conclusions find further support by comparison with the 2 × 1 surface (which we have taken as the known reference for the "weak perturbation" model). In fig. 2b, we observe that the maximum oxygen-induced chemical shift (1.4 eV) on the 2 × 1 surface is clearly smaller than that of the 7 × 7 surface. Fig. 2c shows that annealing transforms the chemical shift to higher value (2.5 eV). The chemical shift of ~3.4 eV, however, is still not developed, in sharp constrast to the case of the 7 × 7 surface where the 3.4 eV shift appeared readily after *room temperature* adsorption. The substantial amount of ~3.4 eV shift observed on 7 × 7 surfaces suggests bonding configuration more closely related to SiO_2 [14].

The lack of difference between valence spectra of the three surfaces (fig. 1) is in clear contrast to the unambiguous difference seen between the Si-2p core level spectra (fig. 2). This contrast demonstrates the superior sensitivity offered by probing atomic levels localized on Si atoms in studying the Si–O system, as has been suggested by Goddard et al. [15] on a theoretical ground. This result also illustrates why early UPS experiments [13] failed to detect differences between oxygen adsorption properties of the 2 × 1 and 7 × 7 surfaces.

Table 1
Summary of the amount of Si atoms involved in bonding to oxygen on different surfaces

Surface	Treatment	Percent of shifted Si-2p	Number of Si bonded to O (in monolayer)
2 × 1	10^3 L O_2	~23	1
	10^3 L O_2 + anneal	~23	1
7 × 7	10^2 L O_2	~35	~1.6

The relative amount of chemically affected Si atoms can be estimated from the relative area under the chemically shifted peaks (fig. 2). The results, expressed as percentage of the total Si-2p intensity, are summarized in table 1. Whereas oxygen coverages are established to be equal on the two surfaces, the numbers of chemically affected Si atoms are clearly more on the 7 × 7 surface. An absolute number of affected Si atoms can also be attempted: if we assume that the 23% shifted Si-2p intensity in the case of 2 × 1 surfaces comes from a full surface layer, the escape depth is calculated to be a reasonable value of 6.5 Å [10]; if only a half monolayer is assumed, an unrealistic escape depth of 2.5 Å is obtained. We therefore in preparing table 1 postulated the number of chemically affected Si atoms to be one monolayer for saturated oxygen adsorption on the 2 × 1 surface. In contrast, the same quantity of adsorbed oxygen affects ~1.6 monolayer Si atoms on the 7 × 7 surface (table 1). The number of ~1.6 monolayer clearly indicates that oxygen has moved beneath the top layer of the 7 × 7 structure. This implies that the backbonds to some surface atoms of this structure are easily broken by the attack of oxygen. Such interpretation is consistent with the presence of the 3.4 eV shift. This oxygen adsorption property should therefore be taken as one strong characteristic of the 7 × 7 structure, and, again, supports the defect models. In general, models within the "defect" class offer an open structure in which oxygen atoms can easily be incorporated into the second layer. For example, oxygen can reach the second layer atoms through vacancies in Lander's vacancy model, or oxygen can attack the relatively exposed backbonds in the adatom structure of either Harrison's adatom model or the milk-stool model, or of the epitaxial bilayer at the microdomain edges in Phillips' model [6]. Here we recognize another advantage of the present technique: while early work measured only the number of adsorbed oxygen atoms, we have also measured the number of chemically affected Si atoms, which is a necessary ingredient for a full determination of the chemical composition of the chemisorption phases.

We can summarize the differences between the oxygen adsorption properties of the 2 × 1 and 7 × 7 surfaces as follows: (i) different oxygen sticking coefficient – it is at least one order of magnitude higher on the 7 × 7 surface. (ii) different bonding configurations – as evidenced by the presence of different chemical shifts and the involvement of unequal number of Si atoms at an about equal oxygen coverage.

A critical implication of the above results is that, in future analyses of the oxygen adsorption process, the role of surface reconstruction has to be included. Although the present finding clearly invalidates the assignment of bonding configuration without distinguishing between the 2 × 1 and 7 × 7 surfaces [12,15,16,17], retention of the reconstructed structure in the final Si–O bonding configuration is not implied. Hence it is possible that, in a more complete theoretical picture, the influence of surface reconstruction on activation barriers of the adsorption process must be taken into account.

It is hoped that the present finding has provided new input for future theoretical and experimental investigations of the 7 × 7 structure. It may also be of importance in developing better understanding of the growth mechanism of practical device oxides, particularly as these oxides become thinner as necessary of very large scale integration (VLSI).

References

[1] The transformation temperature ranges from 200 to 380°C and varies with the density of cleavage steps: P.P. Auer and W. Monch, Surface Sci. 80 (1979) 45, and references therein.

[2] R. Feder, W. Monch and P.P. Auer, J. Phys. C (Solid State Phys.) 12 (1979) L179, and references therein.

[3] This class includes the buckling model of Haneman: D. Haneman, Phys. Rev. 121 (1961) 1093; D.J. Miller and D. Haneman, J. Vacuum Sci. Technol. 16 (1979) 1270; the long range rippling model of Mark et al.: P. Mark, J.D. Levine and H. McFarlane, Phys. Rev. Letters 38 (1977) 1408; and the ring-like arrangement buckling model of Chadi et al. [5].

[4] We realize the imperfect usage of the term "defect" here, because the "defects" we refer to are in ordered positions. However, we will use it to contrast the two types of theory with their relations to an ideal (111) plane. This is the same as what Phillips referred to as "rough" theory [6]. This class includes the point vacancy model of Lander: J.J. Lander and J. Morrison, J. Chem. Phys. 37 (1962) 729; J. Appl. Phys. 34 (1963) 1403; the ad-atom model of Harrison: W.A. Harrison, Surface Sci. 55 (1976) 1; the milk-stool model of Snyder et al.: L.C. Snyder, Z. Wasserman and J.W. Moskowitz, J. Vacuum Sci. Technol. 16 (1979) 166; and the epitaxial microdomain model of Phillips [6].

[5] D.J. Chadi, R.S. Bauer, R.H. Williams, G.V. Hansson, R.Z. Bachrach, J.M. Mikkelson, Jr., F. Houzay, G.M. Guichar, R. Pinchaux and Y. Petroff, Phys. Rev. Letters 44 (1980) 799.

[6] J.C. Phillips, Phys. Rev. Letters 45 (1980) 905.

[7] H. Ibach and J.E. Rowe, Surface Sci. 43 (1974) 481; T. Sakurai and H.D. Hagstrum, Phys. Rev. B12 (1975) 5349.

[8] K.C. Pandey, T. Sakurai and H.D. Hagstrum, Phys. Rev. B16 (1977) 3648, and references therein.

[9] The transition between the fast chemisorption and slow sorption stages is simply termed as saturation: M. Green and K.H. Maxwell, J. Phys. Chem. Solids 13 (1960) 1451; A.H. Boonstra, Philips Res. Rept. Suppl. 3 (1968) 1.

[10] C.M. Garner, I. Lindau, C.Y. Su, J.N. Miller, P. Pianetta and W.E. Spicer, Phys. Rev. Letters 40 (1978) 403; Phys. Rev. B19 (1979) 3944.

[11] A large variation of the oxygen sticking coefficient (3×10^{-4} to 4×10^{-2}) with step density on a 2 × 1 surface was reported by Ibach et al. [12]. However, a more recent analysis of Kasupke and Henzler has shown the variation in sticking coefficient to be less than an order of magnitude (5×10^{-4} to 3×10^{-3}) over the same range of variation in

step density. This new finding is in close agreement with our results. N. Kasupke and M. Henzler, Surface Sci. 92 (1980) 407.
[12] H. Ibach, K. Horn, R. Dorn and H. Luth, Surface Sci. 38 (1973) 433.
[13] H. Ibach and J.E. Rowe, Phys. Rev. B9 (1974) 1951; Phys. Rev. B10 (1974) 710.
[14] G. Hollinger, Y. Jugnet, P. Pertosa and Tran Minh Duc, Chem. Phys. Letters 36 (1975) 441.
[15] W.A. Goddard III, J.J. Barton, A. Redondo and T.C. McGill, J. Vacuum Sci. Technol. 15 (1978) 1274.
[16] R. Ludeke and A. Koma, Phys. Rev. Letters 34 (1975) 1170.
[17] J.E. Rowe, G. Magritondo, H. Ibach and H. Froitzheim, Solid State Commun. 20 (1976) 277.

APPENDIX B

Solid State Communications, Vol. 40, pp. 873–876.
Pergamon Press Ltd. 1981. Printed in Great Britain.

0038–1098/81/450873–04$02.00/0

BONDING OF COLUMN 3 AND 5 ATOMS ON GaAs (110)*

Perry Skeath, C.Y. Su, I. Lindau and W.E. Spicer†

Stanford Electronics Laboratories, Stanford University, Stanford, CA 94305, U.S.A.

Experimental data, in strong disagreement with current theoretical work, shows that the bonding of column 3 elements to GaAs (110) is mainly nondirectional (metallic), with no significant change in GaAs surface lattice reconstruction. Adsorbed Sb, however, is characterized by highly directional bonding. Based on these conclusions, a model of the mechanism of molecular beam epitaxy is presented.

AN UNDERSTANDING of the bonding of column 3 and 5 elements on the surface of 3–5 compounds is important for at least two reasons: (1) the insight given into the electronic structure and chemistry of the semiconductor surface and (2) knowledge of the growth mechanism of these and other crystals. To date, the major contributions have been theoretical [1–5]; however, past history establishes well the necessity of key experimental input in such theoretical calculations. This is due to the large number of possible starting models (e.g. atomic position, nature of bonds, etc.) in such calculations. The limited experimental studies of column 3 elements [4, 6] and 5 elements [6, 7] on GaAs (110) have typically assumed the starting models taken by theorists instead of providing fresh input or real tests of the theoretical models. Here, we report the first major experimental examination on an "atomic" scale of the bonding of column 3 and 5 adatoms on a clean GaAs (110) surface. Most importantly, comparison of theory and our data shows the necessity for a fundamentally different view of the metal–semiconductor bonding.

The GaAs (110) surface is probably the best characterized and understood of all compound semiconductor surfaces and, thus, was chosen for these experiments. The experimental methods have been given in detail previously [8]. Adatoms were evaporated carefully in UHV so as not to heat the room-temperature GaAs surface or to produce contaminants. Thickness was obtained using a dosing technique with a Sloan thickness monitor. Photoemission valence-band EDCs (energy distribution curves) were taken using a CMA (cylindrical mirror analyzer), and LEED (low energy electron diffraction) studies were done with standard 4-grid optics, including $I-V$ curves for Ga and Sb overlayers.

Experimentally, GaAs EDC structure in the upper 5 eV of the valence band have proved particularly sensitive to surface conditions [9]. Theoretical calculations based on models with specific bonding sites have predicted very strong changes in the valence-band structure in this energy range [2–4]. Thus, a careful study of the first 5 eV of the valence band is essential to any understanding of the bonding of column 3 or 5 atoms to the surface. LEED studies provide essential complementary information.

It is now well established that the changes in surface electronic structure due to adatoms can be detected by proper photoemission experiments. In Fig. 1, we present EDCs which examine such changes due to deposition of column 3 (Al, Ga) or column 5 (Sb) on GaAs (110) using $h\nu = 21$ eV. To emphasize any changes produced by the adsorbate (emission from Al or Ga is weak compared to GaAs), Fig. 2 provides difference curves, i.e. the differences between a properly scaled EDC of the clean surface and that obtained after deposition of the indicated amount of Ga or Sb. Also included in Fig. 2 is the surface local density of states (LDOS) calculated by Mele and Joannopoulos (MJ) [3]. Qualitatively similar theoretical results have been obtained by Chadi (C) [4]. In fact, this work was stimulated by these theoretical calculations.

In the calculations of MJ and C, a reasonable assumption of quite localized and directional bonding was chosen in which the column 3 adatom was "covalently" bonded to the semiconductor surface lattice As and/or Ga atoms in a very specific geometry. Not surprisingly, this always produced the type of sharp structure in the surface density of states (SDOS) shown in the calculated curve of Fig. 2, together with large changes in surface lattice reconstruction [10]. A glance

* Supported by DARPA and ONR under Contract Nos. N00014-79-C-0072 and ONR N00014-75-C-0289. Part of the work was performed at SSRL which is supported by the NSF, DMR77-27489, in cooperation with SLAC and DOE.

† Stanford Ascherman Professor of Engineering.

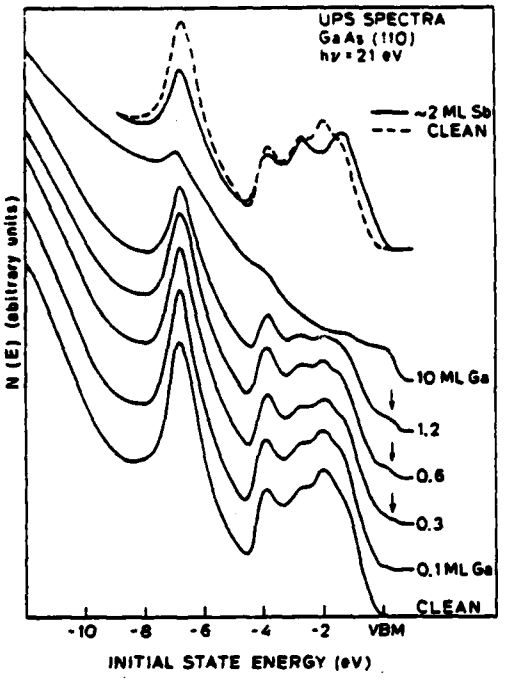

Fig. 1. EDCs of Ga and Sb on *p*-type GaAs (110). Emission from the Ga overlayer (under arrows) is weak due to the large photoemission cross-section of GaAs compared to Ga at $h\nu = 21$ eV.

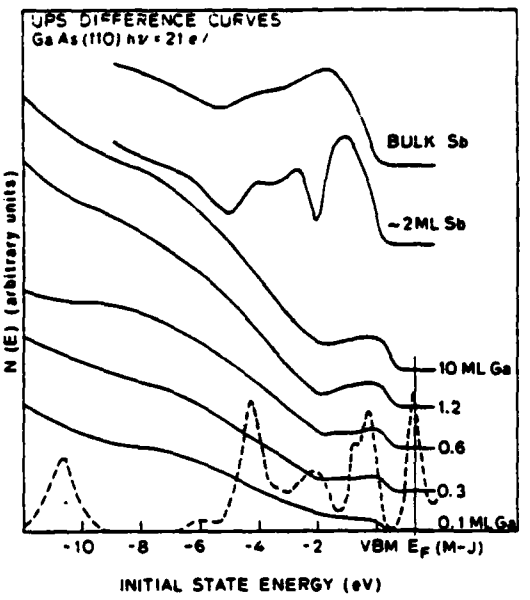

Fig. 2. Difference curves [8] obtained from the data in Fig. 1. The dashed curve overlaying the Ga adatom difference curves is the density of states (DOS) calculated by Mele *et al.* [3] for 0.5 ML Ga on an AlAs (110) surface lattice, with the calculated Fermi level indicated by E_f (MJ). The large number of slow electrons (below -2 eV) in the Ga difference curves is due to MVV Auger and secondary electrons generated by Ga-3*d* core hole decay.

at the experimental curves for Ga will emphasize the extreme difference between our data and these calculations. Similar contrasts between theoretical and experimental results were found for Al on GaAs (110). Thus, it appears that a different model for bonding is needed. Using the data at hand, it is quite possible to make suggestions regarding a new model. However, before doing so, more perspective can be gained by examining the Sb overlayer and the LEED results.

Sb produces quite different results compared to Ga, as can be seen from Figs. 1 and 2. Here, new EDC structure is introduced by the Sb, and GaAs surface-derived EDC structure [9] is altered. As Fig. 2 shows, this is quite different from bulk Sb [i.e. 10 monolayers (ML)]. Intuitively (and consistent with the localized calculations for Ga and Al adatoms), one would expect this to indicate localized orbital-type bonding. This is confirmed by LEED at monolayer Sb coverage which is characterized by a sharp (1 × 1) structure (without increased background) but with $I-V$ curves strikingly different from those of clean GaAs (110) [11]. In contrast, deposition of 0.5 ML Al at room temperature produced an increased LEED background with essentially no changes in translational symmetry, relative spot intensity [8], or in the $I-V$ curves of the LEED pattern [12], indicating a lack of long-range order with column 3 overlayers and no major change in surface lattice reconstruction. At higher temperatures (500°C), the $I-V$ curves are changed, but this is due to a bulk chemical reaction (AlAs formation) beneath the surface and not ordering of chemisorbed Al atoms [12].

At this point, we can conclude that the bonding of the column 5 adatoms to the (110) surface is localized and directional, but the column 3 elements bonding is of quite a different nature. This is plausible since the column 5 elements normally form strongly covalent molecules or solids (bonding dominated by *p* orbitals), whereas the column 3 elements form metallic solids. However, prior work [3–5] has not made this important distinction. Let us next see what can be deduced from the experimental data concerning the nature of the bonding of Ga and Al to the GaAs (110) surface.

First, let us examine the Ga-induced structure of Figs. 1 and 2. We will concentrate on initial energy $E_i > -2$ eV since the strong background for $E_i < -2$ eV, due to an Auger transition, masks the states with $E_i < -2$ eV. The first striking thing is the formation of a well-defined Fermi surface about 0.5 eV above the valence band maximum (VBM), *even at 0.1 ML coverage*. Within 2.5 eV of this Fermi surface,

the EDC is characteristic of an almost free electron metal. This can only be explained by formation of Ga "clumps" – indicative of strong adatom–adatom attraction and sufficient Ga surface mobility. Because of the attenuation of the GaAs EDC structure with increasing Ga coverage, and the strong damping of the localized surface exciton transition [8] at less than monolayer coverage without disruption of other surface electronic structure, we suggest that the "clumping" is predominately two-dimensional at less than monolayer coverage and that the Ga film is of fairly uniform thickness even at 10 ML. Attenuation of LEED spot intensity (by a factory of four) was observed after deposition of 5 Å Ga at room temperature, consistent with a uniform overlayer and 8 Å escape depth. A comparison to deposition of 5 Å Ga at < 100 K, however, suggests the room temperature overlayer is not completely uniform. As with Al [12], no significant change in the form of the $I-V$ curves (single beam) was seen with the Ga overlayer. The two-dimensional aspect of the "clumping" suggests comparable strength in the Ga–Ga (adatom–adatom) and Ga–GaAs bonding.

It is now clear that, for the column 3 overlayers:

(1) Adatom–adatom bonding is a dominant factor, comparable in strength to that toward the crystal (to produce the raft-like almost-free electron metal).

(2) There is no long-range order, i.e. no epitaxy of the Al or Ga on GaAs (110) at low coverage (< 2 ML).

(3) No major changes in the GaAs (110) surface lattice states or reconstruction within the surface unit cell.

These last two facts together are quite striking: they suggest that the bonding of the column 3 atoms to GaAs (110) is predominantly metallic or nondirectional in nature, i.e. that the valence electrons from the Ga adatoms may spend some time in the GaAs without forming a localized highly directional bond. No specific bonding or anchoring site for the Ga clumps or rafts is suggested or indicated by this data. A theoretical understanding of this type of bond is *highly* desirable: How is this bonding accomplished such that the semiconductor surface reconstruction is not affected by the column 3 element overlayer? The conventional approach assuming localized bond orbitals does not seem relevant here.

An equally interesting feature of the data is the strong adatom–adatom interaction. Such a "strong" Al–Al (adatom–adatom) interaction has been found in the calculation by Chelikowsky *et al.* [2]; however, in their calculation, the metal atoms were constrained to epitaxial alignment with the GaAs. Zunger [14] has compared the calculated bond energies of Al on the Ga site [5], Al_2, and bulk Al, and found that three-dimensional cluster formation was energetically favored over single-adatom-per-unit-cell models. Such clusters are known to form at high temperatures. However, two-dimensional rafts may be metastable at room temperature although not the equilibrium state. It is perhaps significant (but not surprising) that jellium overlayer calculations [1] appear to be in better agreement with our results with regard to the density of states of the metallic overlayer.

In contrast to the predominantly metallic Ga overlayer, Sb forms an ordered overlayer due to a more localized and directional bond. Calculations of electronic and lattice structure associated with the Sb overlayer on this basis would be valuable and should result in structures which might, in turn, be checked in detail by LEED or angle-resolved photoemission. Specific models of the ordered Sb overlayer will be examined in a more detailed publication [13].

These results also suggest that, in the growth of epitaxial layers on the (110) face, the first step must be the epitaxial covalent bonding of the column 5 element to the 3–5 crystal. This is in contrast to a view commonly used in theoretical calculations in which the column 3 atom may initiate epitaxy by covalently bonding to the 3–5 semiconductor anion [2–4]. (It should be noted that Goddard [5] has given chemical arguments against bonding of a column 3 adatom to one of the semiconductor surface lattice anions.) Whereas the column 3 metals may not form covalent bonds with the free (110) surface, they are expected to hybridize into an sp^2 or sp^3 configuration, given a site with sufficient neighboring column 5 adatoms. This can be checked using the experimental techniques applied in the present work by depositing a fraction of a monolayer of column 3 (5) followed by a like amount of column 5 (3) atoms. These studies, properly coupled with the theoretical work, indicate a path by which we can begin to study crystal growth mechanisms on an atomic level.

REFERENCES

1. S.G. Louie, J.R. Chelikowsky & M.L. Cohen, *Phys. Rev.* B15, 2154 (1977).
2. J.R. Chelikowsky, S.G. Louie & M.L. Cohen, *Solid State Commun.* 20, 641 (1976).
3. E.J. Mele & J.D. Joannopoulos, *Phys. Rev. Lett.* 42, 1094 (1979).
4. D.J. Chadi & R.Z. Bachrach, *J. Vac. Sci. Technol.* 16, 1159 (1979); and references contained therein.
5. C.A. Swartz, J.J. Barton, W.A. Goddard & T.C. McGill, *J. Vac. Sci. Technol.* 17, 869 (1980).
6. J. van Laar, A. Huijser & J.L. van Rooy, *J. Vac. Sci. Technol.* 16, 1164 (1979).
7. B. Kubler, W. Ranke & K. Jacobi, *Surf. Sci.* 92, 519 (1980).
8. P. Skeath, I. Lindau, C.Y. Su & W.E. Spicer, *J. Vac. Sci. Technol.* 17, 511 (1980).

9. P. Pianetta, I. Lindau, P.E. Gregory, C.M. Garner & W.E. Spicer, *Surf. Sci.* 72, 298 (1978).
10. There is a general consensus among workers in this area that the replacement of Ga in the surface lattice by Al is not expected to have a major effect on the surface lattice reconstruction.
11. P. Skeath, C.Y. Su, I. Lindau & W.E. Spicer, *J. Vac. Sci. Technol.* 17, 874 (1980).
12. A. Kahn, D. Kanani, J. Carelli, J.L. Yeh, C.B. Duke, R.J. Meyer & A. Paton, Presented at the Detroit Meeting of the American Vacuum Society (October 1980) (to be published).
13. P. Skeath, C.Y. Su, I. Lindau & W.E. Spicer, Submitted to *J. Vac. Sci. Technol.*; P. Skeath *et al.* (to be published).
14. A. Zunger (private communication); A. Zunger, *Phys. Rev. B* 24 (Oct. 15 issue, in press) (1981).

APPENDIX C

Solid State Communications, Vol.39, pp.195-198. 0038-1098/81/260195-04$02.00/0
Pergamon Press Ltd. 1981. Printed in Great Britain.

NATURE OF THE VALENCE STATES IN SILICON TRANSITION METAL INTERFACES

G.Rossi, I.Abbati+, L.Braicovich+, I.Lindau, and W.E.Spicer

Stanford Electronics Laboratories, Stanford, California
+permanent address: Istituto di Fisica del Politecnico, Milano, Italy

(Received October 13, 1980 by L.Hedin)

Photoemission spectroscopy using synchrotron radiation and excitation energies around the Cooper minimum have been applied to studies of the nature of the bonding in Si-Pd and Si-Pt interfaces. Evidence is presented that breaking of the tetrahedral coordination in Si and the Si-metal interaction introduces new valence states in the interface region. The energy positron and the orbital character of these Si-metal mixed valence states are determined. A suggestion is made how these results can be generalized to other Si-transition metal interfaces.

The study of the electron states formed in reactive Si transition metal interfaces is receiving increasing attention[1-16] not only for the importance of these interfaces in applications but also for fundamental reasons of interface physics. The behaviour of Si d-metal junctions is dominated by the formation of interfacial reaction products. Correlations between Shottky barrier heights and macroscopic properties of intermixed Si d-metal phases have been pointed out: silicide heat of formation in[17] and silicon metal eutectic temperature in[18]. A step towards the understanding of the fundamental atomic processes underlying these properties is the classification of the nature of the chemical bonds which are formed in the interface region due to the intermixing. This interface work is needed because it is not possible to rely only upon the analogy between interface products and bulk silicide states without limiting the generality of the discussion. It is true that the density of states at the interfaces and in silicides are correlated in many cases[1-3]; nevertheless important differences are found: a concentration gradient is present along the normal to the interfaces[10] and the interface products do not give LEED patterns indicative of single crystal growth unless special treatments are made[15].

The purpose of the present letter is to point out the nature of the valence states in Si-Pd and Si-Pt interfaces. This is the first interface experimental work which gives a comprehensive answer in both cases to this question for the entire valence band range. The conclusions come directly from experimental results without making guesswork based on model calculations for systems with ordered structures. This has been possible by exploiting the unique tunability properties of synchrotron radiation (SR). Thus we have done photoemission measurements at photon energies tuned to the Cooper minimum of the cross section from d orbitals of the metal[9,19]. In this case the d emission is sufficiently reduced that a clear understanding of the sp contributions to the chemical bond is possible directly from the measured photoelectron energy distribution curves (EDCs). We have chosen Si(111)-Pd and Si(111)-Pt interfaces because Pd-4d and Pt-5d have Cooper minima. The present work has also a methodological value since it shows that the Cooper minimum photoemission can be applied successfully to these problems; in this sense the interest of the results is beyond the specific interfaces discussed here. We have done extensive measurements versus coverage (θ in monolayers) but we report here the results only at selected coverages. This is sufficient for the purpose of the present discussion since the dependence is very smooth; a detailed account of the θ dependence will be presented elsewhere[20].

The interfaces were prepared in situ (base pressure 7.10^{-11} Torr) by cleaving n-type Silicon crystals and by evaporating the metal onto the freshly cleaved face held at room temperature. No LEED analysis was carried out onto the Si surface so that nothing can be stated about the quality of the cleave. The evaporation was monitored with a quartz oscillator. The SR light from a "Grasshopper" monochromator[21] was at grazing incidence onto the sample. Angle integrated EDCs were measured with a double pass cylindrical mirror analyzer with the axis normal to the sample surface. The total instrumental resolution was chosen to 0.8-0.9 eV to increase the counting rate at the Cooper minimum where photoemission is very weak. This resolution is sufficiently good for the purpose of the present paper. Some

results on Si(111)-Pd and Si(111)-Pt were also obtained in separate experiments in a vacuum chamber equipped with a LEED apparatus.

The valence photoemission results far from the Cooper minimum ($h\nu$=80 eV) are given in Fig. 1 for Si(111)-Pd at two coverages (θ=0.8, θ=3.2) and for Si(111)-Pt at θ=1.5. With Pd at θ=0.8 a weak 1x1 LEED pattern with an intense background is still seen; in the other cases no pattern is seen so that the interface region does not behave as a crystalline phase in agreement with ref.(15). At $h\nu$=80 (Fig. 1) the d-state cross section is very strong so that the EDCs are dominated by photoemission from these states which are responsible for the main peak around -3 eV with a shoulder at higher binding energies. The EDCs at $h\nu$=80 eV agree with previous results reported in the literature[1,6,11] and taken at different photon energies. In the present case the measurements were done near the minimum of the escape depth so that the information from the first reacted top layer is dominant. We want to stress that the intensity of the photoemission near E_F indicates that a d-contribution is present also at E_F as discussed already in[6]. The reader is referred to this reference for a comparison between photoemission from interfaces and from the pure metals which provides

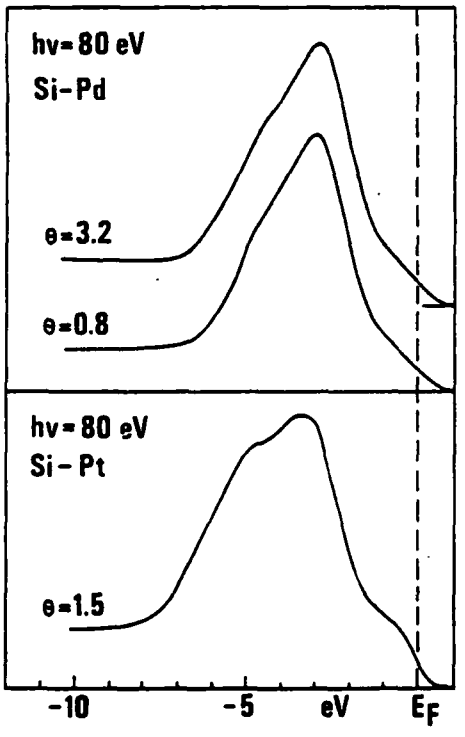

Fig. 1 - Angle integrated photoelectron energy distribution curves for Si(111)-Pd and Si(111)-Pt interfaces at $h\nu$=80 eV. The coverages ( ) are given in monolayer units.

the experimental evidence for chemical reactions at the interface. A deeper insight into the nature of the orbitals in the interface region is obtained by contrasting the photoemission results at lower energies with those at the Cooper minimum. The modification of the EDCs is dramatic and very similar in Si-Pd and Si-Pt interfaces as is shown by the EDCs of Fig. 2 ($h\nu$=130 eV) (solid lines). In these EDCs some d contribution from the metal is still present in the region where the peak is seen at $h\nu$=80 eV. From what is known about d metal cross section[9,19] we can state that at least 40-50% of the emission is from (sp) states in the region indicated by the horizontal bars in Fig. 2; the emission is completely sp below - 7.5 eV. Thus the structures shown in Fig. 2 can provide information about the sp contribution to the orbitals and the role Si plays in bonding to the metal. This role is clear from the comparison (Fig. 2) between the Cooper minimum EDCs from interfaces (solid lines) and from clean Si(111) (dotted lines) measured in the same experiment. Fig. 2 shows a shoulder A at ≈ 1 eV from E_F and a distinct peak C around -10 eV in the spectra from both interfaces. Moreover in the region B (-5-6 eV) the emission is much stronger than in pure Si. The energy position of these distinct features in the interface spectra strongly suggests that A and B contain a considerable amount of Si p oribtal character while C is largely due to s orbitals. Structures A and B are located in a region where strong d orbital contributions from the metal are present as seen from Fig.1 ($h\nu$=80 eV); thus A and B structures indicate the presence of mixed orbitals between Si and the metal mostly via combination of Si p and metal d states. The structure C is outside the d region of the metal; owing to its position it has a (sp) contribution from the metal as it is shown by the increase of C with the coverage. This peak contains Si s electrons which are little involved in the bond. In the high binding energy region of Fig. 2 the EDCs are completely different from that of clean Si(111) which has two structures, while only one is seen from the interface (peak C). The disappearence of the two peak shape characteristic for clean Si is a fingerprint for breaking of the tetrahedral coordination of Si since the double structure is known to be typical of sp^3 configuration in diamond structure. We can thus rationalize the experimental results on the basis of the following density of states structures.

(i) a deep structure C (Si s) little involved in the bonding with sp contribution from the metal
(ii) a region B where mixed orbitals between Si (mostly p) and metal (mostly d) are present
(iii) a main d structure around -3 eV with a shoulder at higher binding energies
(iv) a region A containing mixed orbitals between Si (mostly p) and metal (mostly d); the d contribution extends up to E_F.

The relative position of B and A suggest that B is bonding and A can have antibonding character. We want to emphasize that these conclusions are derived directly from the measurements based on a method which has a

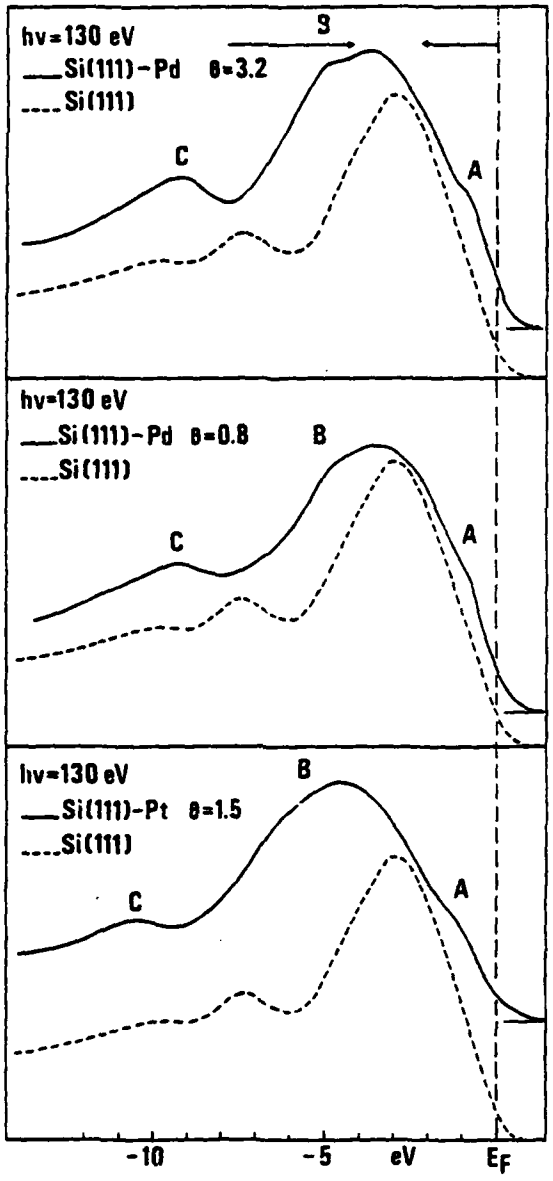

Fig. 2 - Comparison between photoemission spectra at Cooper minimum (hν=130 eV) from Si(111)-Pd, Si(111)-Pt interfaces (solid lines) and photoemission from Si(111) (dashed lines). The coverages are given in monolayer units. The ordinate of the spectra are lower for a factor of ≈ 20 with respect to Fig. 1.

very wide application range. In this respect the present approach is more appealing than Auger lineshape analysis with results very useful in the study of Si-Pd system; in particular our conclusions on states A and B are in qualitative agreement with the Auger work[3] on Pd_2Si, Si(111)-Pd[14] and on Si-Pd glassy metals[22]. Nevertheless the usefulness of Auger lineshape technique in interfaces other than Si(111)-Pd remains to be assumed. Also the calculations on model crystals PdSi and Pd_3Si[3] and on glassy metals[23] suggest a state

classification similar to that presented here.

The analogy between different systems is at first sight surprising and indicates that something common must be present in such situations. One important aspect is probably the breaking of the Si tetrahedral coordination but more research is needed (both experimental and theoretical) to clarify this appealing point. One of the purposes of this paper is to stimulate further work in this direction possibly with a closer connection between structural and spectroscopic investigations.

In conclusion, by using photoemission spectroscopy over a large photon energy range, we have clarified the nature of the valence states in reactive Si/Pd and Si/Pt interfaces. A classification scheme of the different orbital contributions to the bonding is presented which seems to be sufficiently general to be used as a guideline in interpreting future photoemission work on Si-metal interfaces.

Aknowledgments. The authors are indebted to C.M.Bertoni, O.Bisi and C.Calandra and A.Madhukar for very stimulating discussions. I.Abbati is indebted to the University of Southern California for help and assistance; I.Abbati and L.Braicovich aknowledge the support by GNSM of CNR. The work was supported by the Advanced Research Projects Agency of the Department of Defense and was monitored by the Office of Naval Research under Contract No. N00014-79-C--0072. The experiments were performed at the Stanford Synchrotron Radiation Laboratory which is supported by the National Science Foundation under Grant No. DMR77-27489 in collaboration with the Stanford Linear Accelerator Center and the Department of Energy.

REFERENCES

1. J.L.Freeouf, G.W.Rubloff, P.S.Ho, and T.S. Kuan: Phys. Rev. Lett. 43, 1836 (1979).
2. P.S.Ho, T.Y.Tan, J.E.Lewis, and G.W. Rubloff: J.Vac. Sci. Technol. 16, 1120 (1979).
3. P.S.Ho, G.W.Rubloff, J.E.Lewis, V.L. Moruzzi, and A.R.Williams: Electrochem. Soc.Diel.Insul.Electron.Div.Proc. vol. 80-2, 85 (1980).
4. J.L.Freeouf: Solid State Comm. 33, 1059 (1980).
5. J.L.Freeouf, C.W.Rubloff, P.S.Ho, and T.S. Kuan: on print on J.Vac.Sci.Technol..
6. L.Braicovich, I.Abbati, T.N.Miller, S. Schwarz, P.R.Skeath, C.Y.Su, C.R.Helms, I.Lindau, and W.E.Spicer: J.Vac.Sci.Techn. 17, 1005 (1980).
7. I.Abbati, L.Braicovich, B.De Michelis: on print on Solid State Comm..
8. I.Abbati, L.Braicovich, B.De Michelis, U.del Pennino, and S.Valeri: on print on Solid State Comm..
9. J.N.Miller, S.A.Schwarz, I.Lindau, W.E. Spicer, B.De Michelis, I.Abbati, and L. Braicovich: on print on J.Vac.Sci.Technol..
10. I.Abbati, L.Braicovich, B.De Michelis, O. Bisi, C.Calandra, U.del Pennino, and S. Valeri: 15th Conf.on the Phys. of Semicond. (Kyoto, 1980).
11. I.Abbati, L.Braicovich, U.del Pennino, and B.De Michelis: Proc. 4th Int.Conf. Sol.Surfaces (Cannes, 1980). Suppl. "Le Vide, les Couches Minces" n. 201, p.959 and on print on J.Vac.Sci. Technol..
12. I.Abbati, L.Braicovich, U.del Pennino, B.De Michelis, and S.Valeri: ibid.p.1023.
13. I.Abbati, L.Braicovich, B.De Michelis, and M.Sancrotti: ibid.p. 1026.
14. P.S.Ho, H.Föll, J.E.Lewis, and P.E.Schmid: ibid. p. 1376.
15. S.Okado, K.Oura, T.Hanawa, and K.Satoh: Surface Science 97, 88 (1980).
16. P.J.Grunthaner, F.J.Grunthaner, and J.W. Meyer: on print on J.Vac.Sci.Technol..
17. J.M.Andrews, and J.C.Phillips: Phys. Rev.Lett. 35, 56 (1975).
18. G.Ottaviani, K.N.Tu, and J.W.Meyer: Phys.Rev.Lett. 44, 284 (1980).
19. L.I.Johansson, I.Lindau, M.Hecht, S.M. Goldberg, and C.S.Fadley: Phys. Rev. B20, 4126 (1979).
20. G.Rossi, I.Abbati, L.Braicovich, I.Lindau, and W.E.Spicer: to be published.
21. F.C.Brown, R.Z.Bachrach, and N.Lien: Nucl.Instr.Meth. 152, 73 (1978).
22. J.D.Riley, L.Ley, J.Azoulay, and K. Terakura: Phys. Rev. B20, 776 (1979).
23. M.J.Kelly and D.W.Bullet: J.Phys.C 12, 2531 (1979).

APPENDIX D

Oxidation of Si(111), 7×7 and 2×1: A comparison

C. Y. Su, P. R. Skeath, I. Lindau, and W. E. Spicer[a)]

Department of Electrical Engineering, Stanford University, Stanford, California 94305

(Received 7 October 1980; accepted 31 October 1980)

The initial processes of oxygen adsorption on the 2×1 and 7×7 Si(111) surfaces are studied in detail with photoemission techniques. The high-energy resolution and high surface sensitivity Si-2*p* core level spectra have revealed clearly the different nature of the oxygen adsorption processes on the two surfaces. Analysis of the oxidation properties of the 7×7 surface gives strong support for "defect"-type models of the 7×7 structure.

PACS numbers: 79.60. – i, 73.20. – r, 81.60. – j

I. INTRODUCTION

It is well known that the (111) surface of Si exhibits a 2 × 1 structure after cleaving at room temperature, and transforms to a 7 × 7 structure after annealing at elevated temperature (>200 °C). As schematically depicted in Fig. 1, the generally accepted description of the 2 × 1 reconstruction is that rows of surface atoms are alternately raised and lowered.[1] While various models for the 2 × 1 surface differ only quantitatively in the structural parameters describing the "buckling," two qualitatively distinct groups of models have been proposed for the 7 × 7 structure: the "weak perturbation"[2] and the "defect"[3] models. Although we realize the use of "weak perturbation" and "defect" here may raise objections, we hope that the conceptual contrast between the two groups of models are well brought out. As are also illustrated in Fig. 1, the first group of models describes the tendency of the surface to reconstruct within the constraints of the crystal structure, so the final structure is obtained by applying a "perturbation" to the smooth plane. The second group describes the tendency of the surface to break away from the constraints of crystal structure through "defect creation" in the smooth plane.

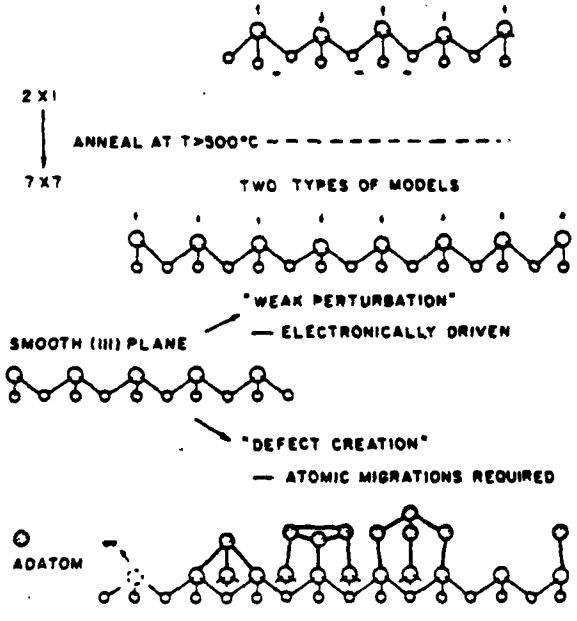

FIG. 1. The surface reconstructions of the (111) surfaces of Si, viewed along a [11$\bar{2}$] direction. Buckling of alternate rows of surface atoms is the generally accepted description of the 2 × 1 reconstruction (top). The two competing types of models for the 7 × 7 structure are contrasted by their relations to a smooth plane. Specific models in the "defect" group mentioned in Ref. 3 are depicted in the bottom schematics.

The great complexity of the 7 × 7 structure has so far prohibited the direct determination of atomic positions through LEED or other experimental techniques. Our approach here is to distinguish the two groups of models through studies of the oxygen adsorption properties of the (111) surfaces. In particular, the 2 × 1 surface will be considered as a "known reference" for the "weak perturbation" model in considering the oxidation behavior.

II. EXPERIMENTAL

The 2 × 1 surfaces were prepared by cleaving *in situ*. The 7 × 7 surfaces were obtained by thermal conversion of cleaved surfaces at temperature ≥500° C. The oxygen exposures were made at room temperature with care being taken to avoid any source of excited oxygen. The photoemission measurements performed are listed in Table I. The 130 eV light source used was synchrontron radiation from the Standard Synchrontron Radiation Laboratory (SSRL). The O-1*s* level was measured with a Mg $K\alpha$ x-ray source.

III. RESULTS AND DISCUSSION

We will compare the 2 × 1 and the 7 × 7 surfaces at the saturation point of the fast chemisorption stage. This point

TABLE I. Summary of measurements.

Measurements	Information gained
Valence structure at $h\nu$ = 130 eV	(1) energy positions of the O-2*p* levels (2) amount of oxygen
Si-2*p* core level at $h\nu$ = 130 eV	(1) oxygen induced chemical shifts (2) number of Si atoms bonded to oxygen
O-1*s* at $h\nu$ = 1253 eV	(1) amount of oxygen (2) binding energy of O-1*s*

 0022-5355/81/030843-04$01.00

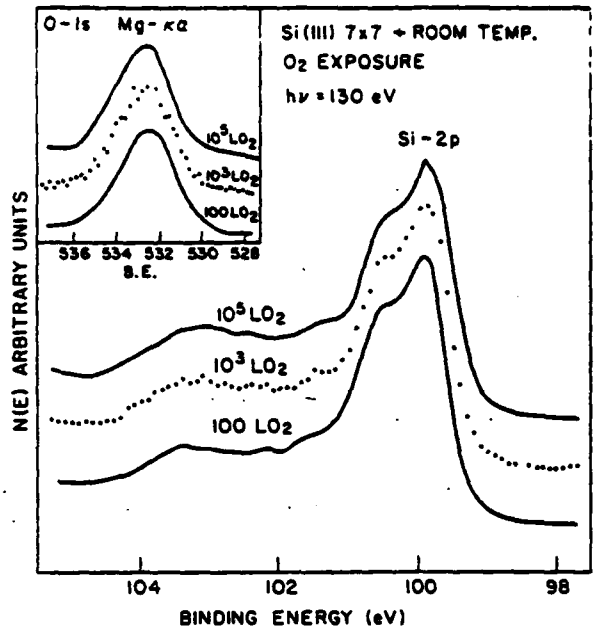

FIG. 2. Si-2p spectra of a Si(111) 7 × 7 surface subjected to a sequence of oxygen exposures at room temperature. The inset displays the corresponding O-1s spectra. Saturation of oxygen adsorption is seen to take place at or below 100 L exposure.

represents the completion of the interaction of oxygen with surface, and hence is useful in revealing the surface structure. Our long experience with the cleaved surfaces has shown that the 2 × 1 surface can be saturated with $\sim 10^3$ L (1 L = 10^{-6} Torr × 1 s) oxygen exposure. This has found close agreement with the recent systematic studies of Kasupke and Henzler,[4] which have also clarified the early finding[5] of a large variation of oxygen sticking coefficient on the 2 × 1 surfaces. The saturation point for the 7 × 7 structure was not as well established in the literature. Hence we show in Fig.

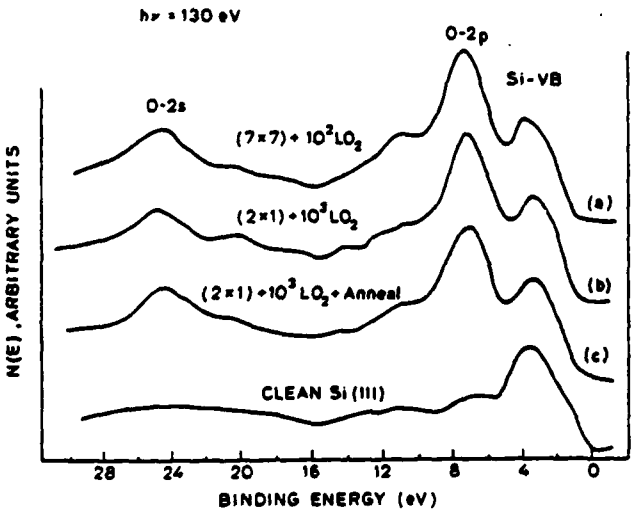

FIG. 3. Valence band region spectra of three different oxygen-covered surfaces. (a) A Si(111) 7 × 7 surface exposed to 100 L oxygen at room temperature. (b) A Si(111) 2 × 1 surface exposed to 1000 L oxygen at room temperature. (c) The surface of (b) annealed at 350° C for ~10 min. The bottom curve is the spectrum of a clean surface.

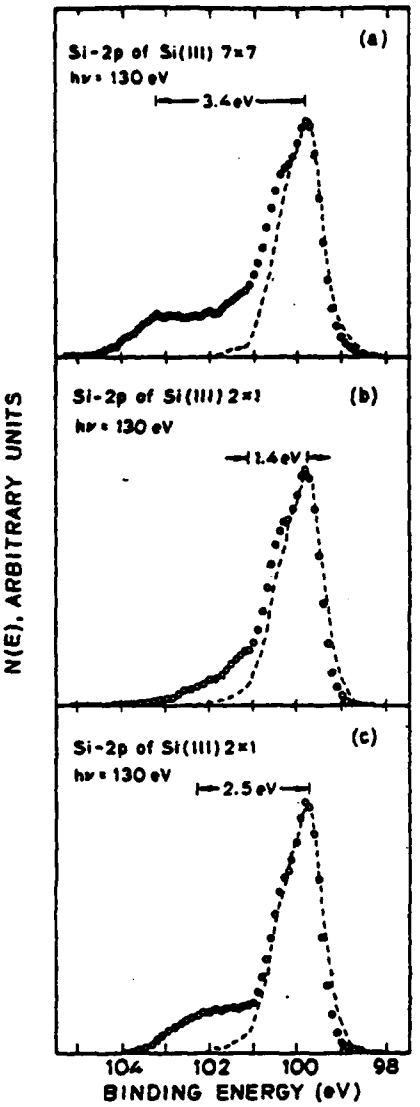

FIG. 4. Si-2p spectra of corresponding surfaces in Fig. 3. The spectrum of the clean surface of each case is shown by the dashed curve.

2 a set of spectra of a 7 × 7 surface subjected to increasing oxygen exposures. Both the O-1s and the Si-2p spectra have clearly established that the saturation exposure is equal to or less than 100 L. Thus the 7 × 7 surface is at least 10 times more reactive to oxygen than the 2 × 1 surface. This difference between the 2 × 1 and 7 × 7 surfaces favors the "defect" models to some extent, because we do not expect such a large difference in chemical reactivity if the two structures are very similar.

Figure 3 gives the valance band region spectra of a 7 × 7 (curve a) and a 2 × 1 (curve b) surface saturated with oxygen. Curve c is the spectrum of a 2 × 1 surface (curve b) oxidized at room temperature and then annealed at 350° C for 10 min. A spectrum of a clean surface is also shown to indicate that the peak at ~3 eV binding energy (BE) is due to Si substrate emission. The peak at 7.3 eV BE is the oxygen nonbonding orbital. We observe the following: (i) The amount of oxygen on the two surfaces are about equal, as measured by the rel-

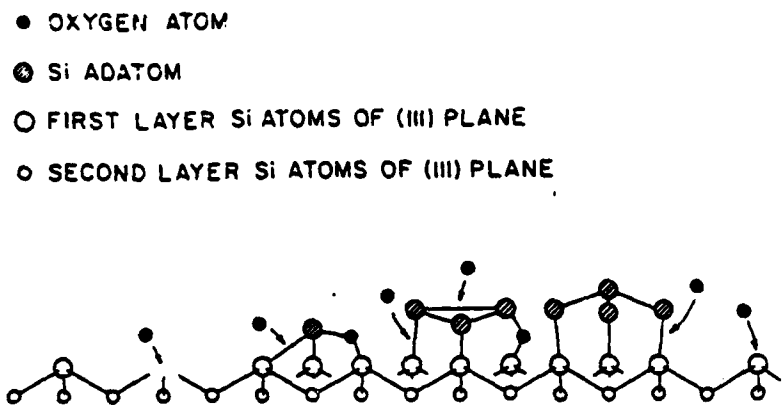

FIG. 5 Schematic illustration of how oxygen atoms can move below the surface layer of the 7 × 7 structures described by "defect" models. The particular 7 × 7 models depicted here are, from left to right, Lander's vacancy model, Harrison's adatom model, the milk stool model, and the epitaxial-bilayer model.

ative peak height of the 7.3 eV BE peak and the 3 eV BE peak. (ii) The valence band region spectra do not reveal significant differences between the two surfaces. This is consistent with the early UPS result.[6,7] The lack of difference in valence band spectra, however, does not imply the same oxidation state for the 2 × 1 and 7 × 7 surfaces, as was concluded in early UPS work.[6] On the contrary, the oxidation states on the two surfaces are distinctly different as found in the Si-2*p* spectra (Fig. 4, to be discussed below).

Figure 4 shows the Si-2*p* core level spectra of the corresponding surfaces of Fig. 3. A spectrum of the corresponding clean surface (dashed) is also included in each case for reference. In Fig. 4(a) we see the presence of several chemical shifts on the 7 × 7 surface, with the highest value of shift being 3.4 eV. This suggests the existence of strongly inequivalent groups of surface atoms in the clean 7 × 7 structure. In the models within the "defect group" we can easily identify such distinctly inequivalent groups, hence this finding is taken as strongly supporting the "defect" type model. This finding is against the "weak perturbation" model, because in a structure close to the smooth plane no such inequivalent groups of atoms can be unambiguously identified; in particular, we cannot identify a special group of Si atoms that can easily achieve, at room temperature, high oxygen coordination number, which is required by the presence of the 3.4 eV shift. The above conclusions can find further support from comparison with the 2 × 1 surface (which we have taken as the known reference for the "weak perturbation" model). Figure 4(b) shows that the chemical shift developed on the 2 × 1 surface after room temperature oxygen adsorption is small (0.9–1.4 eV). Even after annealing this 2 × 1 surface to an elevated temperature, the chemical shift [1.8–2.5 eV, Fig. 4(c)] is still distinctly smaller than what is expected for SiO_2 [3.8 eV (Ref. 8)]. The transformation of chemical shifts in Fig. 4(b) to those in Fig. 4(c) is rather intriguing for understanding the oxidation of the 2 × 1 surface per se, but this will be discussed elsewhere.[9] The important conclusion to draw here is the integrity of the 2 × 1 surface against oxygen attack at room temperature. A similar integrity should be found on the 7 × 7 surface if it were similar to the 2 × 1 surface with nearly identical vertical displacements of the surface atoms (Chadi, Ref. 2).

Another difference between the 2 × 1 and 7 × 7 surfaces is the number of Si atoms bonded to oxygen. These numbers can be obtained by measuring the intensity of the chemically shifted components and by using a reasonable value of the photoelectron escape depth. The percent of shifted Si-2*p* is about ~23% for the 2 × 1 surface both before and after annealing, and is about 35% for the 7 × 7 surface. If we assume that on the 2 × 1 surface there is one monolayer of Si atoms bonded to oxygen, an escape depth of 6.5 Å is obtained.[10] On the other hand, unusual escape depths of 2.5 and 12 Å are obtained, respectively, for assuming $\frac{1}{2}$ and $1\frac{1}{2}$ monolayer of Si bonded to oxygen. Thus it is reasonable to postulate that only the top surface monolayer of Si atoms are bonded to oxygen for the 2 × 1 surface saturated with oxygen. In contrast, the same postulate leads to ~1.6 monolayers of Si atoms bonded to oxygen for the 7 × 7 surface. This number of ~1.6 monolayer unambiguously suggests that oxygen has moved beneath the top layer of the 7 × 7 structure. This is another evidence strongly supporting the "defect" model for the 7 × 7 structure. In general, models within the "defect" group offer an open structure in which oxygen atoms can easily be incorporated into the second layer. In particular, oxygen atoms can access the second layer atoms through vacancies in Lander's vacancy model, or oxygen can attack the relatively exposed backbonds in the adatom structure of either Harrison's adatom model or the Milk-stool model. These ideas are schematically illustrated in Fig. 5. Again, the "weak perturbation" model is disfavored because no special passage for oxygen to reach the second layer can be found in this type structure.

IV. CONCLUSIONS

In conclusion, the present results strongly support a "defect" model for the 7 × 7 structure of the Si(111) surface. We have also demonstrated that, for the same crystalline plane of Si, the two different surface reconstructions can give rise to drastically different oxygen adsorption properties.

ACKNOWLEDGMENTS

Helpful discussions with Professor W. A. Goddard and Professor W. A. Harrison are gratefully acknowledged. Work was supported by the Advanced Research Projects Agency of the Department of Defense and monitored by the Office of Naval Research, under Contract No. N00014-79-C0072 and by the Office of Naval Research, under Contract No.

N00014-75-C-0289. Part of the work was performed at SSRL which is supported by the National Science Foundation Grant No. NSF DMR 77-27489, in cooperation with the Stanford Linear Accelerator Center and the Department of Energy.

[a]Stanford Asherman Professor of Engineering.

[1]R. Feder, W. Monch, and P. P. Auer, J. Phys. C. 12, L179 (1979), and references therein.

[2]This group includes the "key atom" buckling model of Haneman *et al.*, the long-range rippling model of Mark *et al.*, and the ring-arranged buckling model of Chadi *et al.* In the last model, the vertical displacements of surface atoms are nearly identical to those on the 2 × 1 surface: D. J. Miller and D. Haneman, J. Vac. Sci. Technol. 16, 1270 (1979); P. Mark, J. D. Levine, and H. McFarlane, Phys. Rev. Lett. 38, 1408 (1977); D. J. Chadi, R. S. Bauer, R. H. Williams, G. V. Hansson, R. S. Bachrach, J. M. Mikkelson, Jr., F. Houzay, G. M. Guichar, R. Pinchaux, and Y. Petroff, *ibid.* 44, 799 (1980).

[3]This group includes Lander's vacancy model, Harrison's adatom model, the milk stool model of Snyder *et al.*, and the epitaxial-bilayer model of Philips: J. J. Lander and J. Morrison, J. Chem. Phys. 37, 729 (1962); J. J. Lander and J. Morrison, J. Appl. Phys. 34, 1403 (1963); W. A. Harrison, Surf. Sci. 55, 1 (1976); L. C. Snyder, Z. Wasserman, and J. W. Moskowitz, J. Vac. Sci. Technol. 16, 166 (1979); J. C. Philips, Phys. Rev. Lett. 45, 905 (1980).

[4]N. Kasupke and M. Henzler, Surf. Sci. 92, 407 (1980).

[5]H. Ibach, K. Horn, R. Dorn, and H. Luth, Surf. Sci. 38, 433 (1973).

[6]H. Ibach and J. E. Rowe, Phys. Rev. B 9, 1951 (1974); 10, 710 (1974).

[7]Guichar *et al.*, by differentiating high-energy resolution photoelectron yield, have found some difference between the two oxidized surfaces near the valence band maximum. Such minor differences can escape our detection due to the insufficient resolution used here: G. M. Guichar, C. A. Sebenne, G. A. Garry, and M. Balkanski, Surf. Sci. 58, 374 (1976).

[8]C. M. Garner, I. Lindau, C. Y. Su, J. N. Miller, P. Pianetta, and W. E. Spicer, Phys. Rev. Lett. 40, 403 (1978); Phys. Rev. B 19, 3944 (1979).

[9]C. Y. Su, P. R. Skeath, I. Lindau, and W. E. Spicer (unpublished).

[10]This value of escape depth is typical of semiconductors. For example, a minimum escape depth of ~6 Å is found for GaAs: P. Pianetta, I. Lindau, C. M. Garner, and W. E. Spicer, Phys. Rev. B 18, 2792 (1978).

APPENDIX E

Exploiting energy-dependent photoemission in Si *d*-metal interfaces: The Si(111)–Pd case

I. Abbati,[a] G. Rossi, I. Lindau, and W. E. Spicer

Stanford Electronics Laboratories, Stanford University, Stanford, California 94305

(Received 27 March 1981; accepted 14 May 1981)

We present synchrotron radiation photoemission results from Si(111) with increasing Pd coverages θ (in monolayer units from 0.5 to 23 monolayers). We have measured photoemission spectra in the Cooper minimum for the Pd 4*d* electrons ($h\nu = 130$ eV) and outside this region ($h\nu = 80$ eV) where the *d* emission is strong. By comparing the two cases, one obtains information on the Si (*sp*) and Pd (*d*) states. Making use of this, we discuss in detail the coverage dependence of the spectra in connection with the nature of the chemical bond between Si and Pd and the structure of the Si–silicide interface.

PACS numbers: 73.40. – c, 79.60.Eq

I. INTRODUCTION

The study of Si *d*-metal interfaces with electron spectroscopy can provide a wealth of information; in particular, ultraviolet photoemission spectroscopy (UPS) has turned out to be very useful. We have shown recently that the unique tunability of synchrotron radiation (SR) is of tremendous help in these experiments; in fact, very strong modulations of the photoemission spectra take place when the photon energy is tuned through the Cooper minima of the *d* (4*d* and 5*d*) photoionization cross section. The reduction of the *d* contribution in the Cooper minimum makes the Si *sp* contribution clearly visible in photoemission spectra. This allowed us to suggest in a preliminary paper[2] a scheme for the assignment of the orbital nature of the electron states formed in Si–Pd chemical reactions. Interestingly enough, this assignment comes out exclusively from the experimental results without requiring any model calculations. The success of this exploratory work suggested its systematic use in silicide interface problems. This paper is a systematic account on the subject and deals with the results on the Si(111)–Pd interface. Since this is the first systematic application of this approach to silicides, the paper has a methodological value and is primarily intended to show how to exploit energy-dependent photoemission. For that reason, we have selected the Si–Pd interface which is probably the best known and the simplest among reactive Si *d*-metal interfaces. Thus, we will assume that the basic ideas on Si–Pd interface structure consistent with the whole set of published papers are known to the reader. (Recently, a TEM study[18] indicated that the Si/Pd_2Si junction is structurally sharp, with the interface layers characterized by high concentration of structural defects rather than by a ordered intermediate phase). This picture is basically the following for nonannealed interfaces: a rather sharp interface is formed between Si and a reacted product which is Pd_2Si-like. The composition of this silicide is slowly varying along the normal to the interface with a metal concentration increasing away from the interface. At several monolayers of coverage, Si is still present in a metal-rich Si–Pd mixture. We will show that the present energy-dependent photoemission results add important information on the electron states present in these regions and clarify further the nature of the chemical bonds[2] between Si and the metal. Since the aim of the paper is not only methodological, we report also new original information on the Si(111)–Pd interface based on core-line spectroscopy carried out with SR in the low escape-depth region.

The paper is organized as follows. Section II is devoted to experimental considerations and is divided into two subsections: (A) the method, and (B) the techniques. Section III is a summary of the experimental results. Section IV contains the discussion and is divided into three subsections: (A) orbital contributions to the chemical bond between Si and Pd, (B) coverage dependence of valence photoemission, and (C) core-line positions and shapes. The conclusions are summarized in Sec. V.

II. EXPERIMENTAL

A. Method

We have measured photoemission energy distribution curves (EDCs) at increasing Pd coverages deposited at room temperature on cleaved Si(111). This incremental coverage approach is widely used and fruitful, although it is not free of criticism[3] since it does not represent an interface between two semi-infinite media.

The basic idea of the paper is to contrast, as a function of coverage, photoemission results in two cases:

(1) The situation in which the *d* photoemission cross section is dominant over (*sp*) cross sections so that the main contribution to the EDCs is given by the *d* states of the metal (we have selected $h\nu = 80$ eV to get high surface sensitivity).

(2) The case in which the *d* cross section is strongly reduced due to Cooper minimum effect so that a substantial contribution from Si-derived density of states is present in the EDCs (we have selected $h\nu = 130$ eV).

Thus, a hybrid bond formed by the superposition of Si (*sp*) and Pd (*d*) orbitals is sampled in two different ways: in the first case, the *d* contribution is dominant while, in the second case, the *sp* contribution is dominant. The possibility of "switching" from one contribution to another is the key point

 0022-5355/81/030636-05$01.00

and is the consequence of the unique tunability of SR.

At the present time, the above argument on cross sections can not be put in a completely quantitative way since the detailed energy dependence of the d cross section in compounds of this kind is not known. However, the agreement between calculated cross sections for atoms and those found in elemental metals, where $4d$ or $5d$'s form the majority of the valence electrons, is good. The strong reduction of the d emission at $h\nu = 130$ eV found experimentally adds new relevant information on the Si–Pd interface. It should be noted that in ordinary UV experiments (i.e., using He I and He II light), the d-band emission is dominant, as was shown by our preceding results with He I.[4]

In addition to the valence-band photoemission, we have measured at each Pd coverage the Si $2p$ core lines at 160 eV photon energy. This photon energy results in a kinetic energy of the photoemitted electrons where the escape depth is a minimum, i.e., an extremely high surface sensitivity (~5 Å) can be achieved. No Pd core lines could be measured with sufficient signal–to–noise ratios due to the insufficient light intensity at higher photon energies.

B. Techniques

The samples were prepared by cleaving n-type Si crystals *in situ* (pressure in 10^{-11} Torr range) and by depositing increasing amounts of Pd onto the surface at room temperature. The pressure during the evaporation remained in the low 10^{-10} Torr range. The amount of deposited Pd was measured with a quartz oscillator; the coverage θ is expressed in monolayer units, where one monolayer corresponds to 7.8×10^{14} atoms/cm^2, i.e., the Si(111) substrate density.

No instrument was available in the vacuum chamber to characterize the cleave quality—for example, the presence of steps. We can only say that the cleaves appeared flat at visual inspection. Presumably, the cleave quality is particularly important at low coverages. In fact, EDCs from different fresh cleaves may be different, whereas, after deposition of $0.1 \sim 0.2$ monolayers of Pd, the details of the cleave morphology is probably lost and the photoemission spectra are highly reproducible. For that reason, we do not present here results at θ of the order of one-tenth of a monolayer or less.

The EDCs were measured with a double-pass cylindrical mirror analyzer with the axis normal to the surface of the sample and with the SR beam striking the sample at grazing incidence (15°). The light source was the new 4° line at SSRL equipped with a grasshopper monochromator. The overall instrumental resolution (including the photoemission apparatus) was ~1.5 eV at $h\nu = 160$ eV and did not allow the Si $2p$ spin-orbit doublet to be resolved. The EDCs of the present paper have a slightly worse resolution than the preliminary results of Ref. 2; nevertheless, it is sufficient for the purpose of this work. At the Cooper minimum, the typical counting rate was around 100 counts/s for the valence band with the larger slits of the grasshopper (i.e., a factor of 20 lower than at $h\nu = 80$ eV). The calibration of the absolute energy scale of the grasshopper monochromator was not exact; therefore, we give the spectra for the Si $2p$ core lines vs the experimental kinetic energy; the actual binding energy of the Si $2p$ is uncertain by ±1 eV (Fig. 3). The count rate for the Si $2p$ core lines was on the order of 10 000 counts/s, with a signal–to–noise ratio better than 10^2.

III. RESULTS

We present here the photoemission results vs θ in order to point out the main empirical trends. The valence-band EDCs vs θ at $h\nu = 80$ eV are given in Fig. 1 and those at the Cooper minimum ($h\nu = 130$ eV) in Fig. 2. The results of Fig. 1 ("ordinary" photoemission) are in agreement with the results from the literature[4,5,6,14] and show the expected trend in the peak position vs θ. Small discrepancies with respect to other works could be due to the uncertainty in coverage calibration between different experiments and to minor $h\nu$-dependent matrix element effects. The Cooper minimum results are very different from ordinary photoemission as pointed out already in Ref. 2. A relevant feature of the spectra of Fig. 2 is the greater stability of EDC shape at increasing coverages as compared to the results at lower photon energies.[4] At $h\nu = 80$ eV, $\theta = 15$ gives a pronounced shift of the main $4d$ peak, whereas the EDC at $h\nu = 130$ eV is basically unchanged. We will return to this point later in Sec. IV. The Si $2p$ core lines are shown for selected θ in Fig. 3. The emission intensity is plotted vs kinetic energy.

In order to put the empirical trends contained in the above results in better perspective, we present also a plot of the Si $2p$ binding energy shift vs θ (Fig. 4) and of the Si $2p$ and Pd $4d$ intensities vs θ (Fig. 5). The information on the Si emission intensity is more reliable than that for Pd since it is based on

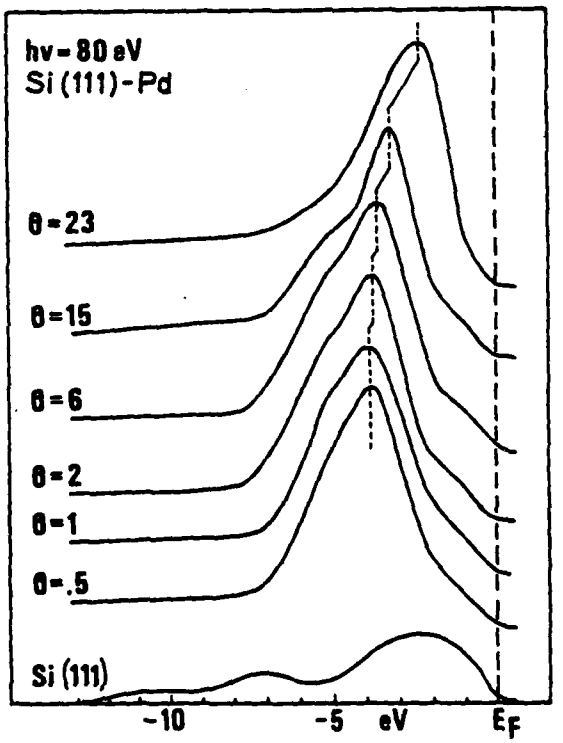

FIG. 1. Angle-integrated photoelectron energy distribution curves at $h\nu = 80$ eV for Si(111)–Pd interfaces at increasing coverages θ, compared with the EDC for a clean Si(111) cleaved surface. The coverages are given in monolayer units.

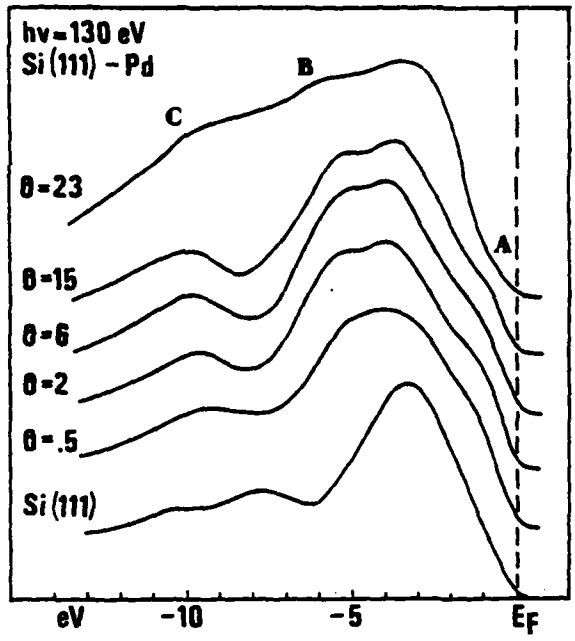

FIG. 2. EDCs at 130 eV, the Cooper minimum, for the Pd 4*d* valence electrons, compared with the Si(111) valence band at the same $h\nu$.

well-defined 2*p* core lines as compared to the Pd 4*d* valence photoemission.

IV. DISCUSSION

The valence-band photoemission spectra at the Cooper minimum show basically constant features over a wide coverage interval. The interpretation of this spectrum (Figs. 1 and 2) is of key importance to the discussion of the interface

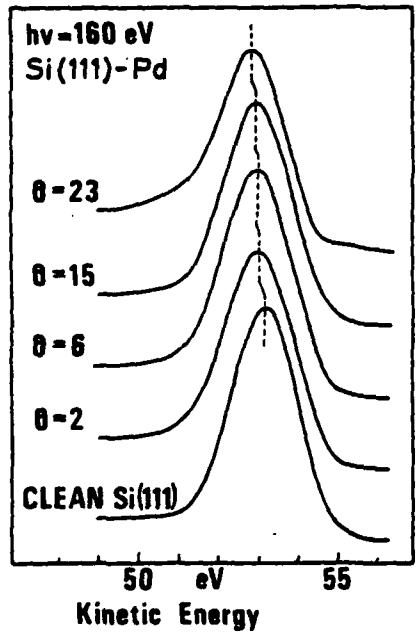

FIG. 3. Si 2*p* unresolved core doublet at $h\nu = 160$ eV for Si(111)–Pd samples at selected coverages. The amplitude of the spectra have been normalized to elucidate the change in line shape and binding energy.

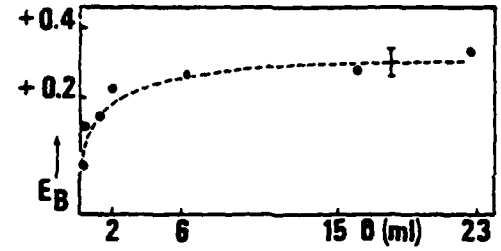

FIG. 4. Si 2*p* binding energy vs Pd coverage diagram; the curve is the best fit of the experimental points.

physics. The Cooper minimum spectrum was already presented and discussed in Ref. 2; therefore, we only summarize the main conclusions in a short paragraph before proceeding to the original information contained in Figs. 1 and 2.

A. Orbital contributions to the chemical bond between Si and Pd

The ordinary photoemission ($h\nu = 80$ eV), the Cooper minimum photoemission ($h\nu = 130$ eV) at $\theta = 0.8$, and the Si substrate photoemission are compared in Fig. 6. Peak C ($h\nu = 130$ eV) originates from Si emission since it is much more evident at the Cooper minimum. This structure is associated with Si *s* states because of its binding energy value. Two extra contributions with respect to pure silicon are evident at the Cooper minimum: the region B below the maximum of the *d* structure and the A structure near E_F. Both structures are in the region where *d* electrons are also present, and this is a strong indication that they are due to hybridization between Pd *d* states and Si states. From the energy position, we can conclude that the Si states are *p*-derived. In the simplest picture, the lower states (B) are associated with bonding and the upper states (A) with antibonding levels. This assignment is also consistent with the theoretical calculations presented in Refs. 8 and 15. It is important to notice that the double-peak structure at −7.5 and −10 eV in clean Si, typical of sp^3 configuration, is replaced by one peak (C in Fig. 6). We take this as direct experimental evidence of the breaking of the tetrahedral coordination of Si upon reaction with the Pd metal. We note that peak C (Si 3*s*) is in the same energy position for both interface products ($\theta \lesssim 6$) and bulk Pd_2Si [sampled at the high coverages ($\theta > 15$)]. The present orbital assignment from Cooper photoemission is consistent with that given in Ref. 15 and obtained with a combination of Auger

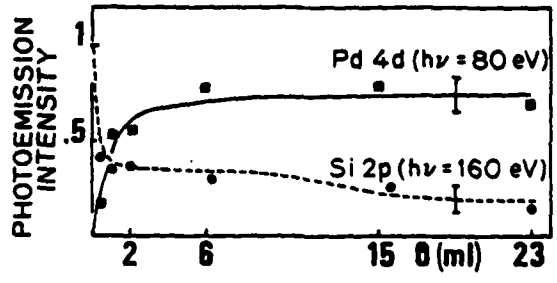

FIG. 5. Si 2*p* signal intensity (dashed line) and Pd 4*d* intensity (solid line) vs Pd coverage; the curves are the best fit of the experimental points.

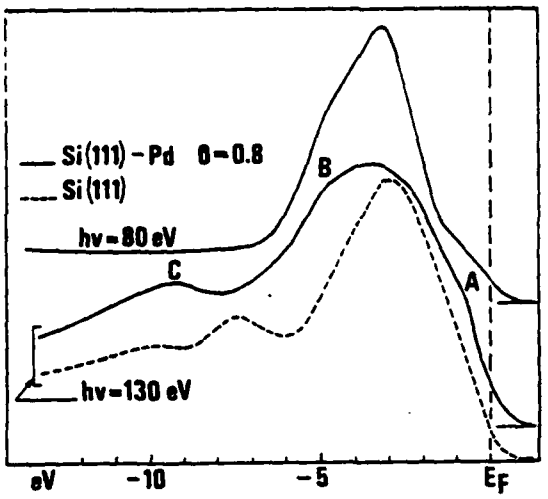

FIG. 6. Comparison of the valence-band EDCs of the Si(111)–Pd interface at 0.8 monolayers for $h\nu = 80$ eV and $h\nu = 130$ eV (Cooper minimum) and the valence band of clean Si(111) at $h\nu = 130$ eV.

line-shape analysis and model calculations. It is encouraging that the results of two independent studies, using different methods, give basically the same result.

B. Coverage dependence of valence photoemission

On the basis of the previous orbital assignments of the main structures of the EDCs, it is possible to point out some relevant information.

(1) The structure around 10 eV below E_F (structure C) increases slowly in intensity with θ ($\theta \leq 6$) and reaches a constant value between $\theta = 6$ and $\theta = 15$. This coverage dependence indicates that structure C is typical of the whole θ interval in which the Pd is almost fully reacted to form a Pd_2Si-like compound on top of the Si(111) surface. The strong reduction of the intensity ($\theta = 23$ in Fig. 2) when the system becomes richer in the metal indicates definitely that the greatest contribution comes from Si electron states. The weak θ dependence at lower θ is the evidence of a small metal contribution to this structure. The metal enrichment at increasing θ is unambiguously shown in Fig. 1 ($h\nu = 80$ eV) by the shift of the main d peak towards lower binding energies. (This is a well-known fact discussed earlier in Refs. 1, 6, and 10.)

(2) When θ increases, the shape of the Cooper minimum EDCs ($h\nu = 130$ eV) is more stable than the ordinary ($h\nu = 80$ eV) photoemission results. At $h\nu = 130$ eV, the EDC at $\theta = 15$ is still basically the same as at smaller θ, while already a considerable shift of the main d peak is seen at $h\nu = 80$ eV, and smaller shifts are seen at lower θ, thus indicating metal enrichment. This point is of paramount importance and can be understood by remembering that the Cooper minimum EDC is related to the local density of states around the Si atoms. Thus, the constancy of the shape of the top 6 eV of the valence band even when the metal concentration increases indicates that the local density of states around Si is not much affected by the increase of the number of Pd atoms and by the change of the above arrangement. The results indicate that the Si local density of states changes dramatically when sp^3 configuration is broken, but it is not very sensitive to the details of the bonds with the metal provided Si–metal (p-d) hybrids are formed. Our data thus provide the first *direct* experimental evidence that the details of the structure are not important as long as Si is completely surrounded by metal atoms. This conclusion regarding the stability of the density of states was also inferred from the model calculations for *bulk* silicides by Ho *et al.*[8] and from the experiments on glassy alloys by Riley *et al.*[15] This "stability" of the local Si density of states can also explain the fact that, at present, the orbital assignment of the structures given in the preceding paragraph seems to work in a variety of cases. For example, this is true for Si–Pt, as was shown by a preliminary measurement reported in Ref. 7 and by extensive research now in progress.[11]

(3) The known metal enrichment at increasing θ and the decrease in Si concentration is particularly evident from Fig. 5. Thus, the Cooper minimum EDC at $\theta = 23$ must be interpreted in terms of metal enrichment effects on the basis of the assignments given in the preceding subparagraph.[7] The decrease of structure C has already been discussed and is easily understood (Fig. 2). At increasing metal concentration, structure A, originating from antibonding (p-d) hybrids, is reduced and obliterated within the noise as a consequence of the decrease in Si concentration. In the meantime, the d contribution to the spectrum (still also present at the Cooper minimum) increases due to the increase in metal concentration. This is explained as the origin of the changes in the EDCs in region B. Since Figs. 1 and 5 clearly indicate that the spectrum characteristic for pure Pd has not been reached, it is not surprising that the d contribution from Pd in region B still resembles that for the Pd_2Si-like situations of bonding (hybridized p-d orbitals). The interesting fact is that the changes of the Cooper minimum EDCs for the metal-rich surfaces are very pronounced. Thus, it should be possible to get more valuable information in this θ range provided a research effort (also theoretical) is made for a more quantitative analysis of the data than has been possible here with the sole use of energy-dependent photoemission data.

(4) Structure A (Fig. 2) is present in the whole θ range up to 15 ML, i.e., up to a coverage where the reaction products are almost silicide-like within the probing depth of the photoemission technique. Within the experimental accuracy, we have no evidence that the intensity of structure A is θ-dependent in this coverage range. In particular, that it is not enhanced at low θ. This is an important observation because the analogous structure examined indirectly in Auger LVV line-shape analysis by G. W. Rubloff *et al.* shows some θ dependence.[6,18] These authors suggest that this might be the evidence for interface states in a fairly abrupt interface between Si and Pd_2Si. On the basis of our experiment, which is much more direct, we find no evidence for this conjecture. Further work with better signal/noise ratio and resolution could be of importance to identify small effects due to coverage dependences. It should also be stressed that considerable uncertainties are also involved in Auger line-shape analysis at low θ.

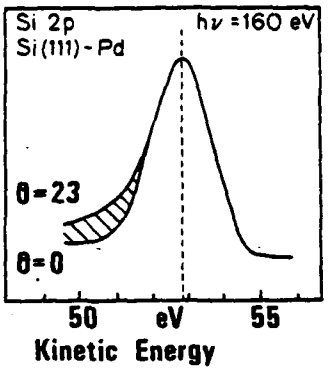

FIG. 7. Si 2p core line-shape variation between the clean Si(111) case and the Si(111) plus 23 monolayers of Pd. The two spectra have been normalized in amplitude and aligned on the energy scale to elucidate the line-shape difference. The dashed area is progressively filled as the coverage of metal increases in the interval from $\theta = 0$ to $\theta = 23$ monolayers.

C. Core line positions and shapes

The discussion of core-line positions is necessarily incomplete since no Pd core line could be measured, while the discussion of the Si 2p core line is very interesting. As far as the core shift is concerned, it is worthwhile noting that the binding energy trend seen in Fig. 3 is consistent with our preliminary results on Si/Pt[11] and those of a related system, Si(111)–Au[1]; recent self-consistent valence states calculations[17] on silicides (Pd_2Si, PdSi) which are related to interfacial compounds show a charge transfer from the metal to silicon.

There are remarkable changes in the line shape of the Si 2p core line upon increasing thickness of the deposited Pd metal. Figure 7 shows a skewed line shape for the unresolved Si 2p doublet at $\theta = 23$. The shaded area in the figure indicates the difference between $\theta = 0$ and $\theta = 23$. No evidence is found that the change in line shape may be due to contaminants. Instead, it appears to be a genuine effect and characteristic for the Sunjic–Doniach line shape[12,13] observed for core levels in metals when pair formation around the Fermi level accompanies the photoemission excitation. However, more experimental and theoretical analysis should be done on the line shape since a certain amount of skewing may also be due to low-energy inelastic losses enhanced by the metallic environment. The skewed line shape at higher coverages is consistent with the increase of available states in the E_F region when the system becomes metal-rich. We have found the same trend in the Si–Pt system vs θ in a detailed experiment carried out under similar conditions as for the Si–Pd system.[11] Thus, the evolution of the Si 2p line shape can be regarded as a typical fingerprint of the changes from a silicide-like interface (where the line-shape modification with respect to Si(111) is small, as shown in Fig. 3) to a metal-rich interface (called "underreacted" in Refs. 6 and 9). To the authors' knowledge, this is the first time that a Si core line has been clearly seen to change from the symmetric shape typical of the semiconductor to that typical of a metal.[16]

V. CONCLUSIONS

We have presented the first extensive application of the Cooper minimum photoemission techniques to studies of the Si–Pd interface. These techniques, combined with the coverage dependence of the photoemission spectra, have made it possible to make a clear assessment of the orbital origin of the electron states formed in the intermixed interface region. In particular, we have followed the transition from a silicide-like region near the interface to a metal-rich region which has electron states still considerably different from those of the pure metal due to the interaction with Si. The Si(*p*)–Pd(*d*) antibonding states near E_F are typical of the silicide-like region and are not seen in the spectra from the metal-rich region; no evidence has been found for interface states in the region between Si and the silicide-like phase.

We have pointed out that in a broad coverage range (up to $\theta = 15$, i.e., beyond the silicide-like region), the local density of states around Si is basically invariant. This was attributed to the breaking of the tetrahedral coordination of pure Si and to a relatively low sensitivity of the local density of states to the details of the structure around the Si atoms.

ACKNOWLEDGMENTS

This work was supported by the Advanced Research Projects Agency of the Department of Defense under Contract No. N00014-79-C-0072.

The experiments were performed at the Stanford Synchrotron Radiation Laboratory which is supported by the National Science Foundation under Grant No. DMR 77-27489 in collaboration with the Stanford Linear Accelerator Center and the Department of Energy.

[a]Permanent address: Istituto di Fisica del Politecnico, Milano, Italy.
[1]L. Braicovich, C. M. Garner, P. R. Skeath, C. Y. Su, P. W. Chye, I. Lindau, and W. E. Spicer, Phys. Rev. B 20, 5131 (1979).
[2]G. Rossi, I. Abbati, L. Braicovich, I. Lindau, and W. E. Spicer, Solid State Commun. (in press).
[3]P. J. Grunthaner, F. J. Grunthaner, and J. W. Mayer. J. Vac. Sci. Technol. 17, 924 (1980).
[4]I. Abbati, L. Braicovich, U. del Pennino, and B. DeMichelis, Proc. 4th Int. Conf. Solid Surfaces (Cannes, 1980); Le Vide Suppl. 201, 959; J. Vac. Sci. Technol. these proceedings.
[5]J. L. Freeouf, G. W. Rubloff, P. S. Ho, and T. S. Kuan, Phys. Rev. Lett. 43, 1836 (1979).
[6]G. W. Rubloff, P. S. Ho, J. L. Freeouf, and J. E. Lewis, Phys. Rev. B 23, 4183 (1981).
[7]L. Braicovich, I. Abbati, J. N. Miller, S. Schwarz, P. R. Skeath, C. Y. Su, C. R. Helms, I. Lindau, and W. E. Spicer, J. Vac. Sci. Technol. 17, 1005 (1980).
[8]P. S. Ho, G. W. Rubloff, J. E. Lewis, V. L. Moruzzi, and A. R. Williams, Proc. Electrochem. Soc. Diel. Insul. Electron. Div., 80-2, 65 (1980).
[9]J. L. Freeouf, G. W. Rubloff, P. S. Ho, and T. S. Huan, J. Vac. Sci. Technol. 17, 916 (1980).
[10]I. Abbati, L. Braicovich, B. DeMichelis, O. Bisi, C. Calandra, U. del Pennino, and S. Valeri, in Proc. 15th Int. Conf. on the Physics of Semiconductors, Kyoto, 1–5 September 1980, edited by S. Tanaka and Y. Toyozawa; J. Phys. Soc. Jpn 49 Suppl. A, 1071 (1980).
[11]G. Rossi, I. Abbati, L. Braicovich, I. Lindau, and W. E. Spicer (to be published).
[12]S. Doniach and M. Sunjic, J. Phys. C. 3, 285 (1970).
[13]G. K. Wertheim and P. H. Citrin, *Photoemission in Solids I*, edited by M. Cardona and L. Ley (Springer-Verlag, New York, 1978).
[14]J. N. Miller, S. A. Schwarz, I. Lindau, W. E. Spicer, B. DeMichelis, I. Abbati, and L. Braicovich, J. Vac. Sci. Technol. 17, 920 (1980).
[15]J. D. Riley, L. Ley, D. Aspnes, and K. Terakura, Phys. Rev. B 20, 776 (1979).
[16]G. Rossi *et al.* (to be published).
[17]O. Bisi and C. Calandra (private communication).
[18]P. S. Ho, P. E. Schmid, and H. Föll, Phys. Rev. Lett. 46, 782 (1981).

APPENDIX F

Proc. 15th Int. Conf. Phys. Semic. (Kyoto, 1980),
J. Phys. Soc. Japan 49 Suppl. A, 1079 (1980).

FERMI LEVEL PINNING AT 3-5 SEMICONDUCTOR INTERFACES*

W. E. Spicer+, P. Skeath, C. Y. Su and I. Lindau

Department of Electrical Engineering
Stanford University, Stanford, California 94305

Using photoemission spectroscopy, the Fermi level at the surface (E_{fs}) can be measured directly as surface conditions are changed. For sufficiently perfect 3-5 surfaces, no surface pinning occurs. As oxygen and metals are added, E_{fs} moves until it takes up a stationary position, E_{fsf}, which is the same for a large number of metals and oxygen and occurs for much less than a monolayer. This and other evidence leads to the identification of a unified mechanism for Schottky barrier and 3-5: oxide interface state formation on the basis of formation of lattice defects. Strong agreement is found with "practical" Schottky barrier and MOS results.

I. Introduction: The Importance of Surface Rearrangement

A *revolution*, based on our ability to study and understand surface and interfaces on a microscopic or "atomic" basis, has taken place. This was triggered by the discovery that the filled surface states on silicon could be studied in detail using ultraviolet photoemission spectroscopy [1], however, many other developments - improved LEED, the availability of synchrotron radiation, etc. - were essential. A key finding was that there are no intrinsic surface states in the the bandgap of GaAs and most 3-5's. Almost simultaneously LEED established strong rearrangement of atoms within the surface unit cell on the (110) surface, with atoms moving by as much as 0.5 Å from their bulk positions. Shortly thereafter, theoretical work completed our first order understanding by definitively showing that the surface states were swept out of the *bandgap region* by this lattice rearrangement [2].

In Figure 1 we summarize these results by schematically showing both the atomic and electronic rearrangement. A fact of prime importance is the realization that rearrangements of atoms, electrons, and electronic states are inextricability interwoven. (Perhaps the most comfortable and familiar bulk analogy is the Jan-Teller effect). On the surface of GaAs and most 3-5's the atoms and electrons rearrange themselves so that the filled surface states move to lower energy below the valence band maximum (VBM) and the empty states to higher energy above the conduction band minimum (CBM). Because the column 3 and 5 elements respectively can de-hybridize toward their atomic configuration with

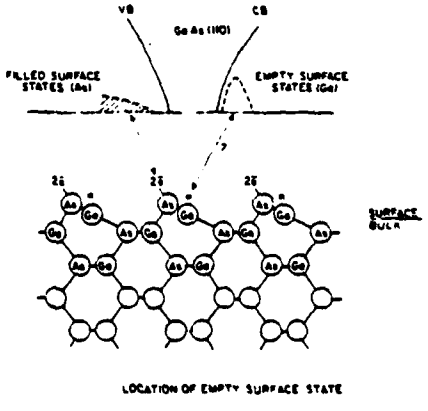

Fig. 1 GaAs surface structure

*Support by ARPA of DOD (monitored by ONR) Cont. N00014-79-C-0072 and by ONR (N00014-75-C-0289)
+Stanford Ascherman Professor of Engineering

3 and 5 valence electrons respectively, the electronic rearrangements for the 3-5's can take place much more ideally than for Si. Thus the surface states are swept completely out of the bandgap. Ga with three valence electrons moves toward a sp^2 (graphite like) bonding scheme with its three neighbors. In contrast, the As surface goes toward a p^3 bonding configuration with the two remaining valence electrons in a s^2 filled non-bonding orbital. The p^3 bond angle is more acute than the bulk sp^3 covalent bond, thus moving the As atom outward. In contrast, the sp^2 Ga bond is almost planar pulling the Ga inward (see Fig. 1) [2,3]. Note that there are no "dangling" bonds in the classical sense. The As "S^2" electrons are available for bonding; however, if the "S^2" arrangement is thus changed the surface will rearrange at that point, inducing additional strain [2].

In the past a very elementary picture of the inter-relation of intrinsic surface and bulk states has been popular. The bulk electronic and lattice structure was throught to extend right up to the vacuum-semiconductor interface and then surface electronic states were added in the bandgap at the surface. The inadequacies of this are now apparent. The lattice structure generally changes as we move to the surface. It is unlikely that these changes are completely restructed to the last layer of the semiconductor [2]. The large atomic rearrangements must lead to large changes in the electronic structure associated with the surface. Thus, our older models (and even that of Fig. 1 insofar as it is interpreted in those terms) must be abandoned and we must think in terms of a lattice and thus, electronic structure which are unique to the surface region. This is reflected in recent theoretical work which calculates the local density of states layer by layer as one moves from the surface into the bulk [4].

The rearranged surface atoms are not lattice matched to the bulk crystal. This results in distortion of the bulk lattices for at least one additional layer of atoms beneath the surface. Because of the lattice mismatch, a large strain field can be expected in the outmost surface layers. The difference in crystal structure within the surface unit cell should produce a surface lattice vibrational structure different from the bulk. This will be important in explaining observed phenomena in this paper.

A key concept which has been brought into focus by the removal of surface states from the bandgap region (Fig. 1) is the distinction between intrinsic and extrinsic surface states. Intrinsic refers to the states characteristic of the perfect (albeit rearranged) surface. In contrast, the extrinsic states are those due to defects, either structural or impurities, at or near the surface. The extrinsic bulk states are of such importance because they dominate the electrical and thus the practical applications of semiconductors. This would be a very obscure meeting, were it not for practical implications of the basic work reported here; however, it is not the surfaces of semiconductors but their interfaces with, for example, metals and insulators that are of practical importance. There is a critical point which we must test. Are the extrinsic states, created by perturbation of the clean surface by the sub-monolayer quantities of foreign atoms, pertinent to the states determining the electric characteristics of interfaces between the semiconductor and the thick metal or oxide layers characteristic of practical devices? A prime objective of the research described here was to determine whether such a connection exists.

Let us now be more explicit in outlining our objectives. They are: (1) to determine the extrinsic surface state formed in the bandgap by deposition of oxygen or metallic atoms; (2) to attempt to determine the nature of extrinsic surface states so created; (3) to see if such states are relevant to the states which form the interface states governing the electrical properties of metal: or oxide: semiconductor interfaces; (4) to see if a new and difinitive model for Schottky barrier height and 3-5: oxide interface states can be developed. The change of the surface Fermi level (E_{fs}) with increasing surface perturbation (produced for example, increasing the number of foreign atoms placed on the surface) gives information on the energies and density of the extrinsic states so induced.

II. Measurement of the Surface Fermi Level Position and Other Comments on Experimental Techniques

Photoemission provides a method of directly measuring E_{fs} [5]. The essence of such a measurement is shown in Fig. 2. In the lower part of the figure we indicate schematically the band structure of a metal (Au) and semiconductor (GaAs); however the semiconductors with identical bulk doping have different densities of extrinsic surface states. For the semiconductor in the middle, this density is sufficiently low so that the surface and bulk Fermi level positions are the same; for the semiconductor on the right, the extrinsic surface state density is large enough to pin E_{fs}. In our experiments we started with an unpinned surface for either an n- or p-type sample, perturbed the surface by deposition of a metal or oxygen, and measured the movement in E_{fs} (see Fig. 3). As shown in Fig. 2 a downward movement of the surface Fermi level (E_{fs}) produces an equal upward movement of the valence band maximum and other valence band structure such as the sharp peak near the bottom of the EDC. If E_{fs} moves downward by an amount $-\Delta E_{fs}$, the valence band structure (or core levels - which are often accessible) moves up by an equal amount. In this way E_{fs} can be located to ± 0.1 eV or better. The photon energy is chosen so that the structure originates only from the last few layers of the semiconductor, whereas the band bending extends over a much larger distance. Thus, we determine the EDC's changes and E_{fs} at the surface.

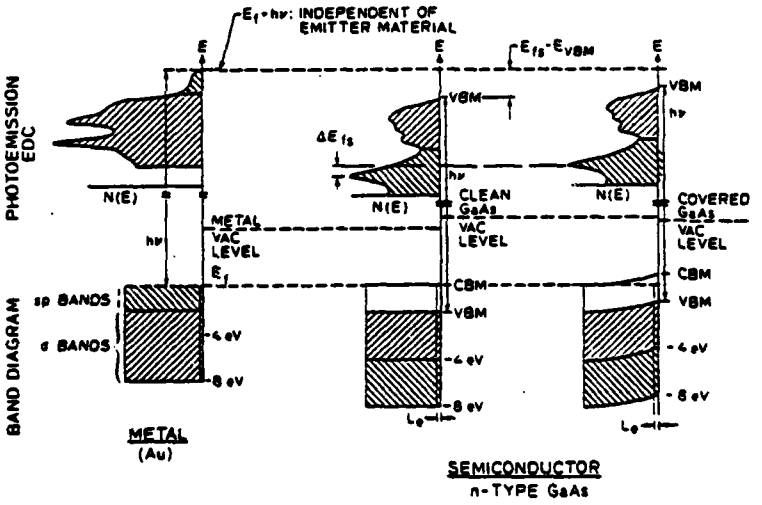

Fig. 2 Determination of E_{fs}

The reader is warned against experiments (such as Kelvin prove measurements) which measure the work function (rather than E_{fs}) as metals or oxygen are added to the surface. The work function depends not only on E_{fs} but also on the electron affinity, E_A, which will also change. Error may develop because of the difficult in separating changes in these two parameters. Data exists in the literature in which unreliable means have been used to make this separation. Data so obtained and conclusions drawn therefrom are not reliable [6].

The surface Fermi level measurements were essential to these studies. However, they were not sufficient. Critical to these studies and the insights presented in this paper are a wide range of photoemission data using tunable synchrotron monochromatic radiation as a photon source. The unique capabilities

provided by synchrotron radiation are given in detail elsewhere [2] and will not be described here. We will also make use of Sputter-Auger data. Considerable effort has been spent at Stanford in refining these techniques.

One thing common to all of our photoemission measurements is that we can limit the depth sampled in photoemission measurements to the last two or three layers of the semiconductor. This is done by choosing a photon energy of the excited electrons to place them in the minimum of the escape depth versus kinetic energy curve for GaAs or other 3-5's. The escape depth versus kinetic energy curve is available in the literature [8]; it has a broad minimum of about 5 Å centered about 60 eV.

III. Changes of E_{fs} on GaAs, InP, and GaSb(110) due to Adatoms

The largest single surprise that came from this work was the realization that oxygen and metals pinned *the surface* Fermi level at approximately the same position. This is illustrated by Fig. 3 where the movement of E_{fs} for n- and p-type GaSb is plotted as metals or oxygen are added to the surface. Note that the shape of the curves and the final pinning positions, E_{fsf}, are similar [7]. In Fig. 4 E_{fsf} is given for a number of metals and oxygen on InP, GaAs, and GaSb. The accuracy of these positions is ± 0.1 eV or better. For these measurements to be possible the clean surface must be prepared in such a way that the extrinsic surface state density is sufficiently low (less than 10^{11}-10^{12}/cm^2) so that it does not measurably affect the position of E_{fs}. Only by cleaving in ultra-high vacuum have such surfaces been obtained to date [2]. These results are striking in that E_{fsf} depends strongly on the semiconductor but not on the adatom even though these adatoms span the electronegativity curve (from Cs through Au to oxygen). This is a key finding and we will return to it often in using our data to understand the physics and chemistry taking place. Another critical point is the coverage at which E_{fsf} is obtained. This is as little as 0.1 of a monolayer (Ml) for metals and even less for oxygen. This again will be very important in understanding the mechanisms of Fermi level pinning.[9]

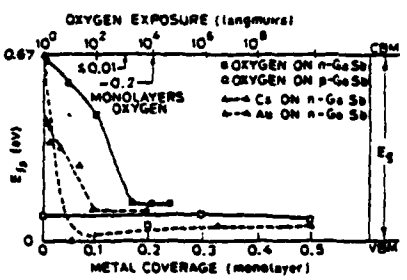

Fig. 3 E_{fs} vs. coverage

IV. The Mechanism of Fermi Level Pinning

The pinning takes place at coverages where many adatoms are acting almost as as individual atoms. How can atoms with such different atomic orbitals induce

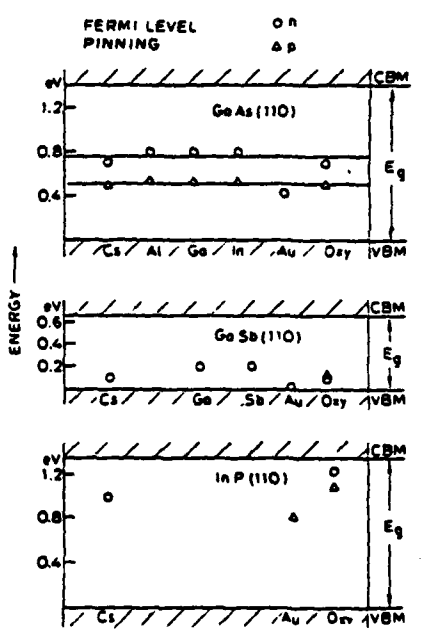

Fig. 4 E_{fsf} vs. adatom

states which has identical energy [8]? Reflection leads to this: the adatoms do not directly produce the extrinsic surface states; rather, they indirectly induce the states which do the pinning. Logic indicates that the induced states are lattice defects such as vacancies or defect complexities due to vacancies. We believe it is most likely that the defects lie just below the surface. Theory suggests that the energy of the defect will depend on its position with regard to the surface for the first one or two surface layers and then will reach a constant value independent of position. If the defect were on, or sufficiently near the surface, it would be expected to interact with the surface impurities and thus the energy level would depend strongly on the identity of the adatom; this is not seen. The defects formed in this study are probably the simplest which are stable, i.e. immobile at room temperature since they were formed under the most "gentle" conditions available to us with the crystals at room temperature [2,5]. (It is very important that future studies be made as a function of temperature.) For the metals, the evaporator was well away from the crystal and depositions were made for short times to avoid long exposure of the crystal surface to the thermal radiation of the deposition system. There was no evidence that the average temperature of the crystal surface rose appreciably during deposition. The oxygen is added using great care that only "unexcited" oxygen is used, i. e. oxygen in the molecular ground state. It is now well-established that the "excited" oxygen not only can increase the sticking probability of the oxygen but in some cases - e.g. GaAs - can drastically change the surface chemistry [10]. Using the E_{fsf} (Fig. 4) and other inputs, we have derived the energy level diagram (in Fig. 5) for the extrinsic surface states. Also indicated are our suggestions as to the electrical classification of the levels (i.e. donor or acceptor) and the missing atom responsible for the defect.

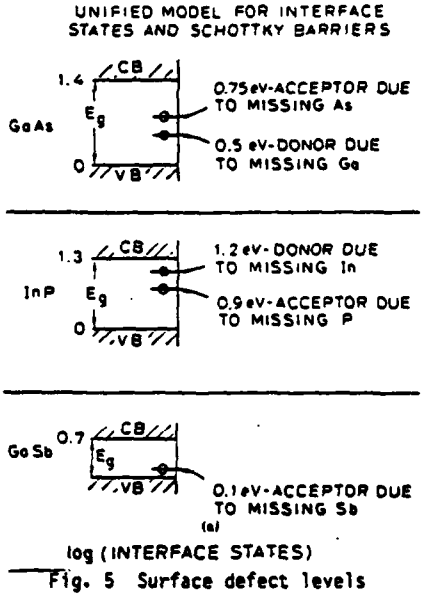

Fig. 5 Surface defect levels

The most difficult and uncertain task (except for GaSb) is determining the identity of the missing atom which gives rise to a given energy level. For Sb, the choice was easy: (1) because the removal of Sb from GaSb due to deposition of the metal was so apparent and (2) because an energy level at the same position as that reported here had long been established to be due to the missing Sb atom. The complex is generally thought to consist of a Ga in a Sb site "tied" to a nearest neighbor Sb vacancy [2] To make the assignment for As, we note that pinning is often observed on clean cleaved n-type GaAs sample [2]. However, it is less common to find any pinning on a cleaved p-type sample. Arguing that one is much more likely to lose As than Ga in the cleaving process, we associate the 0.7 eV level with a missing As. The identity of the levels in InP is even more difficult. Our suggestion was parallel with the well established GaSb case and our identity of the 0.7 eV GaAs state, i.e. missing column 5 elements (at least under our conditions produce acceptors). We found additional support from the work of others [9]. However, Williams et al [11] have come to the opposite conclusion from ourselves as to the missing atoms [12]. Considerable theoretical work is underway [13]. This confirms the general trends shown in Fig. 4 and 5. However, the calculations are very difficult for a number of reasons and detailed agreement between experiment and theory can not be claimed.

V. Mechanism of Defect Formation

That lattice defects may be formed by oxide growth has long been recognized. As we will discuss later there is reasonable correlation between energy level positions found in this work and those at the interfaces of such thick device oxides. However, we find the formation of these levels by only a few percent of a Ml of oxygen. Further, there is strong evidence that the oxygen is in the form of a surface "chemi-adsorbed" species rather than bulk oxides [2]. Thus, we must suggest a mechanism which can occur under these conditions as well as for thicker oxides. It is now essential that the reader review Fig. 1 and Section I to recall the remarks made about surface lattice strain inherent in the clean reconstructed surface. We will continue that discussion by mentioning that it has been established that the sharpness of the surface valence band gives a sensitive measure of the crystalline perfection of the surface [14]. The occurrence of pinning of the Fermi level at the surface is the most sensitive test of surface perfection. For cleaved surfaces, there is a strong correlation between E_{fs} pinning and reduced surface valence band EDC sharpness [15].

The E_{fsf} occurs at roughly the point at which surface "valence band" disorder occurs, i.e. the sharp valence band structure abruptly disappears [2]. LEED studies as a function of oxygen exposure (taking care to use only unexcited molecular oxygen) shows that the first layer of atoms becomes disordered with less than a monolayer of "chemi-adsorbed" oxygen [16]. Return again to Fig. 1 and realize that, if oxygen removes electrons from a surface As atoms as experiments clearly show, As will attempt to form a new band configuration. This may add a new, local strain field to that already present. The surface valence band and LEED data indicate that this additional strain is enough to disorder the surface. One mechanism for relief of strain is the creation of lattice defects. E_{fs} movement shows that this clearly begins to occur well before the surface disorders [15]. The correlation with "thick" oxides interfacial energy levels indicates similar levels are produced in that case.

For deposited metals, there is no intrinsic need for semiconductor material to be incorporated into the ad-layer. The textbook model of a Schottky barrier has usually assumed a completely abrupt junction between the semiconductor and metal. Our studies (example of which is given in Fig. 6) show that this is not the case. Remembering that our photoemission experiments sample only the first few layers at the surface, we see in Fig. 6 that the d-core levels of both semiconductor components (Ga and Sb in this case) are clearly seen on the clean surface. The Ga intensity falls off as Au is deposited (although much slower than for an abrupt junction) and the Sb intensity is little diminished even for thick metallic layers (suggesting surface segregation of Sb). The results for GaAs and InP were similar with the exception that no strong preferential surface segregation effects were seen. These core studies were confirmed and additional information was given by Sputter-Auger studies [17]. The experiments ruled out the possibility of artifacts due to "pinholes" or other nonuniformities in the films.

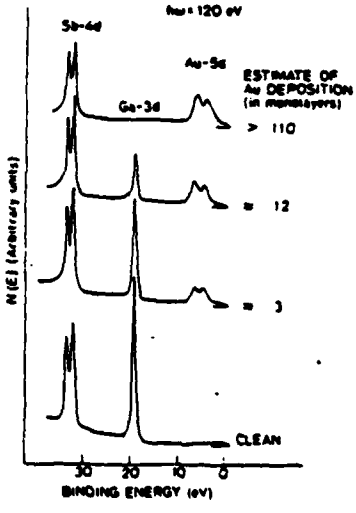

Fig. 6 Au on GaSb

Covalent semiconductor bonds must be broken in order to move semiconductor atoms into the metal. What provides the activation energy for this? The bulk phase diagram does not favor such movement for a number of the systems investigated. Note also that the E_{fsf} is reached with much less than a monolayer of metal, again arguing against bulk compound formation. Only when we realized that the heat of adsorption of the metals is comparable to or larger than covalent bond energies did a possible explanation emerge. It should be recognized, at once, that the heat of adsorption is a purely surface quantity and cannot be predicted in terms of the bulk heat of formation or reaction. For example, Cs forms no strong compounds with Ga or As but the heat of adsorption of a Cs atom on a clean GaAs surface is over 60 K cal/mole ($\sim$3 eV). In contrast the heat of condensation of Cs on bulk Cs is only about 20 K cal/mole ($\sim$1 eV). There is a lack of direct information on the heat of formation for the systems of interest. Only for Cs are precise numbers available. However, the indirect evidence suggests that the heats of adsorption are high, e.g. over 90 K cal/mol. (4 eV) for Au [2] on 3-5 compounds.

Figure 7 shows the detailed mechanism we propose to explain both the intermixing and defect formation during metal deposition. The heat of adsorption produces a local small "thermal spike". Due to the surface strain and surface-bulk phonon mismatch, an atom is occasionally ejected (about 1% occurence), producing a defect. Because of the care with which the foreign atoms are added to the surface, we probably are dealing with the simplest stable defect. Subsequent heating or "hot" depositions could produce larger and more complicated defect centers; however, as will be discussed in the next section, it appears that the resulting energy levels are only shifted by a small amount (usually less 0.2 eV). In InP, where the donor lies above the acceptor, Williams et al [11] and Farrow et al [8] have obtained striking results.

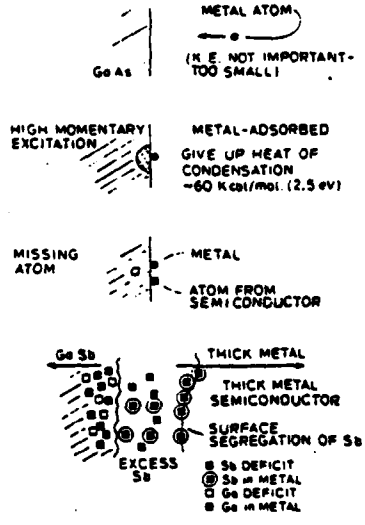

Fig. 7 Defect formation mechanism

VI. Correlation with Device Structures and the Unified Model

The values of E_{fsf} (for metals see Fig. 5) are in surprisingly good agreement with those found previously from Schottky barrier heights [2,9]. There is also surprisingly good agreement between E_{fsf} (Fig. 5) and the oxide: 3-5 interface states [2,9,19]. This has led to the formalization of a unified mechanism for the formation of Schottky barriers or the 3-5: oxide interface states [9]. It is unified because, to the first approximation, the same lattice defects provide the dominant energy levels. This also clears up a long standing mystery for 3-5 Schottky barriers. In contrast to Si, 3-5 Schottky barriers are surprisingly insensitive to the surface conditions before metal deposition, i.e. to air, the presence of a few layers of oxide, as opposed to atomically clean starting surfaces. Since (as has been established in this work) the same defect levels and thus E_{fsf} are provided by oxide and the metals for 3-5's, there should be little sensitivity to surface oxide as is observed.

The inversion of the acceptor and donor defect levels on InP, make E_{fs} on

this material very sensitive to the relative number of acceptor and donor defects [9, 12,20]. In practical structures, it is found that changes in processing can change the dominate defect level and thus the Schottky barrier [11,18] height on InP or the dominate defect level [21] for InP: oxide (MIS) structures. Both effects are well documented [9,11,12,18,21]. In Fig. 8 we indicate the defect levels we deduced for InP and the interface state density found [21] using CV techniques by preparing InP MIS structures in different ways [12,21]. Good agreement is obtained between our results and the observations for the MIS devices [12].

Fig. 8 is presented to highlight another effect discussed at the end of Section 5. We believe that we have identified the simplest stable defects. In real processing more complex defects may be formed or the simple defects may be distorted by strain, etc. Thus, in practical cases, one tends to see rather continuous distributions of states rather than simple delta functions as might be expected if only the simplest stable defect levels were present [12].

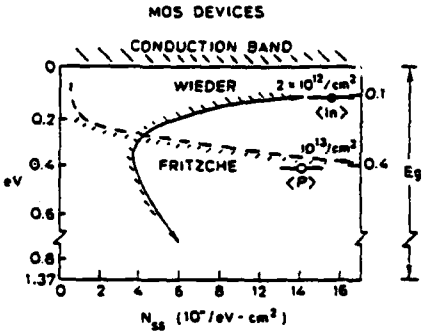

Fig. 8 Interface states-MOS device

In conclusion, studies of E_{fs} combined with other measurements have allowed us to develop an understanding of 3-5 surface and interfaces on an atomic level. A critical result is the realization that the 3-5: metal or oxide interfaces are not ideal but are dominated by the same defects. Thus, a Unified Model has been developed to explain both Schottky barrier formation and gap states at 3-5: oxide interfaces. Although these details could not have been deduced previously because of the lack of sufficient experimental data, Phillips [22] is rather unique among theorists in predicting the importance of the metallurgical and chemical interactions at the interface.

References

[1] L.F. Wagner and W.E. Spicer, Phys. Rev. Lett. 28 (1972) 1381; Phys. Rev. B 9, (1974) 1512
D.E. Eastman and W.E. Grobman, Phys. Rev. Lett 28 (1972) 1378.

[2] An excellent view of these developments can be obtained from the Proceedings of the Physics of Compound Semiconductor Interfaces, published as J. Vac. Sci. and Tech. 13, No. 4 (1976); 14, No. 4 (1977); 15, No. 4 (1978); 16, No. 4 (1979); and 18, No. 5 (1980); in view of this the number of individual references will be drastically limited.

[3] J. Barton, W. Goddard III, and T. McGill, J. Vac. Sci. and Tech. 16, (1979) 1178, and ref. therein.

[4] See invited papers by J. Chadi and M. Cohen in these Proceedings and ref. therein.

[5] P. Skeath, I. Lindau, P.W. Chye, C.Y. Su and W.E. Spicer, J. Vac. Sci. and Tech. 16 (1979) 1143.

[6] L.J. Brillson, R.Z. Bachrach, R.S. Bauer, and J. McMenamin, Phys. Rev. Lett. 42, and ref. therein.

[7] C.M. Garner, C.Y. Su, W.E. Spicer, P.D. Edwood, D. Miller, and J.S. Harris, Appl. Phys. Lett. 34 (1979) 610.

[8] P. Pianetta, I. Lindau, C.M. Garner, and W.E. Spicer, Phys. Rev. B 18 (1978) 2792.

[9] W.E. Spicer, I. Lindau, P. Skeath, C.Y. Su, and P. Chye, Phys. Rev. Lett. 44 (1980) 420, and references therein.

[10] P. Pianetta, I. Lindau, P.E. Gregory, C.M. Garner, and W.E. Spicer, Sur. Sci. 72 (1978) 298.
[11] R.H. Williams, R.R. Varma, and A. McKinley, J. Phys. C 10 (1979) 4545; T. Humphreys, M. H. Patterson and R.H. Williams; J. Vac. Sci. Tech., Oct.-Nov. (1980) in press, and ref. therein.
[12] W.E. Spicer, I. Lindau, P. Skeath, and C.Y. Su, J. Vac. Sci. and Tech., Oct.-Nov. (1980) in press.
[13] M.S. Daw and D.J. Smith, J. Vac. Sci. and Techn. 16, Oct.-Nov. (1980) in press and ref. therein;
M. Nishida, Surf. Sci., in press.
[14] P. Skeath, W.A. Saperstein, P. Pianetta, I. Lindau, W.E. Spicer and Peter Mark, J.Vac. Sci. Tech. 15 (1978) 1219.
[15] W.E. Spicer, P. Pianetta, I. Lindau, and P.W. Chye, J.Vac.Sci. 14 (1977) 885.
[16] A. Kahn, D. Kanani, P. Mark, P.W. Chye, C.Y. Su, I. Lindau and W.E. Spicer, Sur. Sci. 87 (1979) 325.
[17] P.W. Chye, I. Lindau, P. Pianetta, C.M. Garner, C.Y. Su, and W.E. Spicer, Phys. Rev. B 18 (1978) 5545.
[18] R.F.C. Farrow, A.G. Cullis, A.J. Grant and J.F. Patterson, J. Crystal Growth 45 (1978) 292.
[19] W.E. Spicer, I. Lindau, P. Pianetta, P.W. Chye, and C.M. Garner, Thin Solid Films 56 (1979) 1.
[20] P.W. Chye, C.Y. Su, C.M. Garner, P. Pianetta and W.E. Spicer, Sur. Sci. 88 (1979) 439.
[21] H.H. Weider, pa. 234; D. Fritzche, pa. 258, Inst. Phys. Conf. No. 50, Ed. by G.G. Roberts and M. J. Morant (The Institute of Physics; Bristol (1980).
[22] J.C. Phillips, J.Vac. Sci. and Tech. 11 (1974) 947;
J.M. Andrews and J.C. Phillips, Phys. Rev. Lett. 35 (1975) 56.

APPENDIX G

3rd Symposium Appl. Surf. Anal. (1980), to be published in Applic. Surf. Sci.

ABSTRACT

A Unified Model for Schottky Barrier Formation and MOS Interface States on 3-5 Compounds

W. E. Spicer, I. Lindau, C. Y. Su and P. Skeath
Department of Electrical Engineering, Stanford University
c/o Stanford Electronics Laboratory, Stanford, CA 94305, U.S.A.

The object of the work reported here has been to develop an understanding on an atomic basis, of the interaction between semiconductor and metals or oxygen overlayers which determine the electronic characteristics of the interface, e.g. the Schottky barrier height of metal-semiconductor interface or the density and the energy position of oxide-semiconductor interface states.

The principal experimental tool used has been photoemission excited by monochromatized synchrotron radiation ($10<h\nu<300$eV). Extreme surface sensitivity is obtained by tuning the synchrotron radiation so that the minimum escape depth is obtained for the excited electrons of interest. In this way only the last two or three atomic layers of the solid is sampled. By changing $h\nu$, core levels or the valence bands can be studied. Using a metallic reference, the Fermi level position at the surface, E_{fs}, can be directly determined.

GaAs, InP, and GaSb have been studied. On a proper cleaved surface, there are not surface states in the semiconductor band gap; thus, no pinning of E_{fs}. Pinning of E_{fs} can then be monitored as metals or oxygen are added to the surface--starting from sub-monolayer quantities. Two striking results are obtained: 1) pinning position is independent of adatom for oxygen and a wide range of metals, and 2) the pinning is completed by much less than a monolayer of adatoms. These results can not rationally be explained by the pinning being due to the levels produced directly by the adatoms. Rather, they suggest strongly that the adatoms disturb the semiconductors surface forming defect levels. This is supported by appearance of the semiconductor atoms in the metal and by the disordering of the semiconductor surface by sub-monolayer quantities of oxygen. Since these basic experiments have been reported previously they are only reviewed briefly here.

When metals or oxygen are added under very gentle conditions, the following levels are formed (all energies relative to the conduction band minimum).

III-V	Acceptor(Missing Atom)	Donor(missing Atom)
GaAs	0.65 eV (As)	0.85 eV (Ga)
InP	0.45 eV (P)	0.1 eV (In)
GaSb	0.5 eV (Sb)	below VBM (Ga)

These results explain why Schottky barrier gates will provide useful FET's on n-GaAs but not n-InP. Likewise they predict that MOS or MIS gates will be practical for n-InP but not n or p GaAs. Studies of the oxygen surface chemistry find the As oxides to be unstable and P oxides to be stable--reinforcing the prediction. Recent work of others is reviewed and alternate identification of the missing atoms in the defects is discussed. Some of the new process possibilities opened up by this work are considered.

THE UNIFIED MODEL FOR SCHOTTKY BARRIER FORMATION AND MOS+ INTERFACE STATES IN 3-5 COMPOUNDS

W. E. Spicer*, I. Lindau, P. R. Skeath, and C.Y. Su
Dept. of Electrical Engineering
Stanford University
Stanford, CA 94305

I. Introduction

As much of the material in our oral presentation at the 3rd Symposium on Applied Surface Analysis has been published, it would be inappropriate for the written version of the publication to reproduce that material. Rather, this paper will have five purposes:

1) to briefly outline the experimental data which lead to the development of the "unified" model,
2) to briefly summarize the "unified" model,
3) to outline recent work of others both theoretical and experimental related to the "unified" model,
4) to show how critical choices on devices can be made (using present device technology),
5) to point out ways that the limitations inherent in (4) might be changed by new device processing technology.

+ Work supported by ARPA under contract No. N00014-79-C-0072 and ONR under contract No. N00014-75-0289.

Part of the experiments were performed at the Stanford Synchrotron Radiation Laboratory which is supported by the National Science Foundation under Grant No. DMR77-27489 in cooperation with the Stanford Linear Accelerator Center and the Department of Energy.

* Stanford Ascherman Professor of Engineering

II. Experiments Which Resulted in Development of the "Unified Defect Model"

A range of conventional experimental techniques including LEED[1], Auger (the use of Auger was minimized because of the electron beam damage to the surface), and UPS[2,3] with conventional sources were used in this work. However, the use of synchrotron radiation from the Stanford Synchrotron Radiation Laboratory (SSRL)[4] for UPS ($10 < h\nu < 200$eV) was essential to this work, since the tunability of synchrotron radiation made possible key experiments involved examining core and valence levels of the last one or two molecular layers of the semiconductor at the surface.[5-8]

Another critical technique was the direct measurement of the surface position of the Fermi level, E_{fs}, by photoemission.[7,8,9] It should be emphasized that we directly measured E_{fs}. Such measurements should be distinguished from those of others[10] who have measured changes in work function and attempted to deduce E_{fs} from these and auxiliary measurements.

On a "well cleaved"[2] (110) surface of most 3-5 compounds, E_{fs} is not pinned since rearrangement of the near surface atoms move the intrinsic surface states out of the band gap,[6-8]--thus one can start with a surface where E_{fs} is at the bulk Fermi level position. Both n-type and p-type crystals, with near degenerate doping levels, were used so that the Fermi energy on the clean surface was near to one of the band edges. Then by adding foreign atoms such as oxygen and metals and watching the movement of E_{fs} until it becomes pinned, one can determine the new energy levels induced at or near the surface.

The key results from this study were the findings: 1) that the E_{fs} pinning position was essentially independent of ad-atoms, i.e.

it was at the same position independent of whether the ad-atom was a metal (Cs, Al, In or Ga) or oxygen (see Fig. 1b), and 2) that the pinning was stabilized by much less than a monolayer of the ad-atom (see Fig. 1a). On this basis, the popular theories of Schottky [6-8,12] barrier formation could be discarded (however, the results were in the direction suggested by Phillips and co-workers[11]). Since the ad-atoms must all be inducing the same surface or "near" surface states, the only reasonable conclusion was, that these states were due to a structural defect produced by the perturbation due to the ad-atom on the surface lattice.

It should be noted that the free surface was highly strained by the rearrangement which moved the intrinsic surface states out of the band gap.[13] It is well established that oxygen adsorption disorders the surface lattice--a process in which defects would be expected to be produced.[6,13] With metal ad-atoms, experiments at SSRL monitoring the core levels of the components of the 3-5 compounds showed that on deposition of many monolayers of the metal, the column 3 and column 5 constituents of the semiconductors moved into the metal.[6-8,12] A detailed mechanism which provides the activation energy for this has been suggested.[6-8,12]

As will be seen in the next section, others have since found independent support for the defect model. It is formally titled the "Unified Defect Model", since it simultaneously explains Schottky barrier formation and the origin of the 3-5: oxide interface states in MOS or MIS structures as being due to the creation of the same defect states.

Making use of the movement of E_{fs} with deposition of ad-atoms[6-7],

the defect levels in Fig. 2 have been deduced. The energy positions are considered to be quite firm within the experimental error of ± 0.1 eV; The defect type (n- or p-) is also considered quite certain (a n-type surface defect level can donate an electron to the bulk whereas p-type surface defects can accept an electron from the bulk. In GaAs and InP the origin of the defect associated with the energy level, (e.g. a defect due to a missing As in GaAs,) is considered quite tentative. Other suggestions which have been made by Williams[15] for InP, and by Harrison[16], Grant et al,[17] and Monch et al[18] for GaAs are also indicated in the caption of Fig. 2. The identity of the defect for GaSb is thought to be quite certain as it agrees with that for bulk GaSb[19].

The energy levels shown in Fig. 2 also agree as well as can be hoped for with Schottky barrier heights and oxide:semiconductor interface levels found in device structures.[6-8,12] It should be noted that, while all of our measurements were made on the (110) cleavage face (the crystal were cleaved in situ at 10^{-10}torr), most of the device structures were made on (111) or (100) faces of the 3-5's. The theoretical work of Daw and Smith[20] shows that, if the defect levels lie two or more molecular layers beneath the interface, they will be characteristic of the bulk and thus not depend on the crystal surface. The experimental results mentioned above suggest that this is the case as do other arguments[6-8,12]

It should be emphasized that the metal ad-atoms in our experimnets were deposited as gently as possible (by evaporation) and that the crystals were not heated during or after deposition. The defect formed may be vacancy or defect complexes as in the case of GaSb[19] (i.e. "clusters" of two or more defects). Heating or other treatment may change a vacancy into a complex or change the nature of a complex. However, if this is happening

for the defects of interest here, the energy levels are changed by only small amounts (of the 0.1eV), because the Schottky barrier heights and positions of MOS interface states agree so well with results obtained in devices processing where the samples are not treated so gently.

III. Recent Work of Others

As mentioned above, we are in agreement with Williams et al[15] for InP except for the assignment of the missing species producing the defect. There is also agreement with Farrow et al [6-8] in the location of the InP defect energy levels.

The theoretical work of Daw and Smith[20] based on a simple As vacancy gives the observed systematics, as well as insight associated with the vacancy levels as it is moved from the surface into the bulk.

Wieder[21] has studied the Fermi level pinning position by measuring the highest filled level in MIS structures in the system $Ga_xIn_{1-x}As$ (n-type) as x is increased from 0 to 1. He found that he could explain his data if he assumed that the pinning was due to a anion vacancy level which was at a fixed height, 0.53eV, above the valence band maximum, independent of the composition of the $Ga_xI_{1-x}As$. The result of a constant vacancy level due to an anion vacancy level is in agreement with recent ab initio calculations of Daw and Smith[22] for the alloy system.

Gatos and co-workers,[23] making use of the GaAs-oxide interface states in a "photo-transitor" mode, have detected directly the level near 0.7 eV. Monch et al,[18] measuring the charge in contact potential of a GaAs surface as a function of temperature, have located both GaAs defect levels shown in Fig. 2 and find agreement with our energy asignments. Making certain assumptions, they deduce from their data (as indicated in Fig. 2) that the levels shown in Fig. 2 are both due to the same defect associated with

a missing As atom. The defect can either accept an electron or a hole in agreement with the theoretical consideration of Harrison[16] and interpretation of their own data by Grant et al[17].

Considerable work is underway on the defect model. For good collections of articles, the reader is referred to the Proceedings of the Eighth Conference on the Physics of Compound Semiconductor Interfaces[24] (and the Proceedings of the 15th International Conference on the Physics of Semiconductors[25]. Of particular interest are some of the theoretical work of Allen and Daw[24] who suggest that a surface anti-site defects are responsible for the interface pinning. The calculations of M. Nishida[25] and the measurements of H. Hasegawa and T. Sawada[25] should also be noted.

IV. Critical Device Choices Which Can Be Made In Context Of Existing Process Technology

An extremely important consequence of the "Unified Defect Model" and the energy levels shown in Fig. 2 is the choice of the type of gate for FET's made with GaAs and InP. Because the energy levels of GaAs lie near mid-gap, it forms relatively high Schottky barriers and thus provide good Schottky barrier gates for FET's (Skeath et al[26] have recently showed that even larger barrier heights may be possible on n-type GaAs). However, the depth of the defect levels make GaAs very unfavorable for MOS application. This problem is compounded by instability of the As-oxides[27,28].

Because of the position of the defect levels in InP if near the conduction band minimum it gives too small a Schottky barrier height for a practical Schottky gate on n-type InP. However, the low activation energy of the interface defect levels on n-type material makes it a good candidate for MOS or MIS devices. The fact [28,29,30] that there is not the instability

problem for P-oxides which exists for As-oxides makes this model of operation even more encouraging. In fact, Wieder,[31] Meiners,[32] and co-workers[33] have obtained very promising results in MIS operation of InP devices.

In conclusion, if the results of the "Unified Defect Model" are applied to making choices for FET configurations for InP and GaAs using existing device processing, it is clear that GaAs could be only be expected to work for Schottky barrier and not MOS or MIS gates. This is in agreement with the practical experience, i.e. the success with Schottky barrier gates and failure (despite heroic efforts) with MOS or MIS (it should be remembered that all existing MIS structures have a thin oxide layer on the seiconductor surface before the insulator is deposited) structures. Conversely, there has been no success with InP Schottky gates but increasing success with MIS structure on InP[31-33].

V. New Device Possibilities

Once one knows the source of a given phenomena, new techniques can be envisioned to modify or eliminate that phenomena. Knowing that Schottky barrier formation and 3-5:oxide interface states are both due to the same defects opens two closely related avenues. For example, to modify the Schottky barrier pinning position methods one might reduce the defect density and/or add dopants in the surface or interface region in large enough quantities to overcome the effect of defects.

The work of Farrow et al [28,34] in which the Schottky barrier height of Ag-InP(100) was studied as a function of stoichiometry of the (100) face illustrates the second point given above. If the polar face was saturated with P before depositing the Ag, the Schottky barrier height was found to

be very small (~0.1eV below the conduction band minimum, CBM) in accord with the donor level shown in Fig. 2 However, if no special treatment were given the InP face prior to deposition of the Ag, the normal barrier height of ~0.4eV was obtained in agreement with the acceptor level in Fig. 2 Clearly the saturation of the surface with P has inhibited the formation of the level 0.4 eV below the CBM (which we attribute to missing P) with respect to the 0.1 eV level (which we attribute to missing In).

In Fig. 1c we present what we believe to be the first clear example of a dopant overwhelming the defect levels at the interface of a 3-5 semiconductor. In our previous studies[6-8,12] we have found that the Au gave a pinning position on n-type GaAs somewhat nearer the valence band maximum (VBM) than any of the other metals (or oxygen) studied (see Fig. 1b) Therefore we determined to study Au in more detail. The results of Skeath et al [26] in Figure 1c give the results in terms of E_{fs} as a function of the amount of Au deposited on an atomically clean GaAs (110) cleavage face. The curve for p-type GaAs is most instructive. At low coverages the E_{fs} rises as it typically does for metals on GaAs (see Fig. 1a. However, whereas the metals normally level (Fig. 1a) off at the final pinning position given by Fig. 2, a reversal takes place with Au, i.e. after E_{fs} reaches a maximum, it monatomically decreases with increasing Au coverage. This indicates that two competing mechanism involved in pinning E_{fs}. At low coverages the defect mechanism dominates; at higher coverages, the acceptor level (lying near VBM) introduced directly by Au (probably by Au moving into the GaAs) clearly overcomes the defect levels and determines E_{fs}. An important factor for Au moving into GaAs is the atomically cleanliness of the starting

GaAs surface. It appears that even a few layers of oxide greatly inhibits this movement. Such layers are always present in "practical" GaAs-Schottky barrier made on GaAs surface which have been exposed to the air. This is the reason that this effect has not been clearly seen previously.

In the discussion above we give two examples of the methods by which the Schottky barrier height can be changed in real devices. These should be taken as somewhat crude examples having been discovered without the intention of controlling the barrier height. Making use of techniques such as MBE, one can hope to design structure giving the desired behavior and then develop processes to realize it. For example, one might learn how to heavily dope the last ten or twenty layers of n-type InP with an acceptor, e.g. Be or Zn, to make it strongly p-type. The InP growth would then be terminated with In and a metal deposited to form a Schottky barrier. This metal may be an alloy containing In and appropriate heating schedules might be developed. In this way, the formation of donors due to missing In would be minimized and E_{fs} will be determined by the Be or Zn acceptors which lie near the VBM. In this way, a Schottky barrier height almost equal to the band gap could be obtained on n-type InP--something which has not proven possible to date.[8,12] In fact, the inability to form a satisfactorily high Schottky barrier on InP has impeded the practical application of this material greatly.

The above gives just one of many configurations which can be envisioned based on the understanding of the fundamentals of Schottky barrier and 3-5: oxide interface formation material as outlined earlier. It should also be noted that certain questions (see Section II) remain as to the

details of the defects involved. These questions need to be cleared up definitively to give the firmest knowledge possible for the "scientific" engineering of new, improved device structures.

REFERENCES

1. Perry Skeath, W. A. Saperstein, P. Pianetta, I. Lindau, W. E. Spicer and P. Mark, J. Vac. Sci. and Techn. 15, 1219 (1978).

2. P. Pianetta, I. Lindau, P. E. Gregory, C. M. Garner, and W. E. Spicer, Sur. Sci. 72, 298 (1978).

3. C. Y. Su, I. Lindau, P. R. Skeath, P. W. Chye and W. E. Spicer, J. Vac. Sci. Tech. 17, 936 (1980).

4. I. Lindau and W. E. Spicer, Chpt. 6 in Synchrotron Radiation Research ed. by H. Winick and S. Doniach, Plenum Press, N.Y. 1980 and ref. therein.

5. Ibid, pp. 162-167.

6. W. E. Spicer, P. W. Chye, P. R. Skeath, C. Y. Su, and I. Lindau, J. Vac. Sci. Tech. 16, 1422 (1979); I. Lindau, P. W. Chye, C. M. Garner, P. Pianetta, C. Y. Su, and W. E. Spicer, J. Vac. Sci. Tech. ibid, 15, 1332 (1978).

7. W. E. Spicer, P. W. Chye, P. R. Skeath, C. Y. Su, and I. Lindau, Inst. Phys. Conf. Ser. No. 50, pp 216, Ed. by G. G. Roberts and M. J. Morant, The Inst. of Physics, Bristol, 1980, and ref. therein.

8. W. E. Spicer, P. Skeath, C. Y. Su, and I. Lindau, Proc. 15th Int. Conf. Physics of Semiconductor, Kyoto, 1980, J. Phys. 49, (1980) Suppl. A, pp. 1079-1087.

9. Perry Skeath, I. Lindau, P. W. Chye, C. Y. Su, and W. E. Spicer, J. Vac. Sci. Tech. 16, 1143 (1979).

10. L. J. Brillson, Phys. Rev. B18, 2431 (1978); L. J. Brillson, R. Z. Bachrach, R. S. Bauer, J. C. McMenamin, Phys. Rev. Lett. 42, 397 (1979) L. J. Brillson and D. W. Kruger, Sur. Sci. 102, 518 (1981) and ref. therein.

11. J. M. Anderson and J. C. Phillips, Phys. Rev. Lett. 35, 56 (1975) and ref. therein.

12. W. E. Spicer, I. Lindau, P. Skeath, C. Y. Su, and P. Chye, Phys. Rev. Lett. 44, 420 (1980) and ref. therein.

13. W. E. Spicer, P. Pianetta, I. Lindau, and P. W. Chye, J. Vac. Sci. Tech. 14, 885 (1977).

14. P. Chye, I. Lindau, P. Pianetta, C. M. Garner, C. Y. Su, and W. E. Spicer, Phys. Rev. B18, 5545 (1978).

15. R. H. Williams, R. R. Varma, V. Montgomery, J. Vac. Sci. Tech. 16, 1418 (1979); T. Humphreys, M. H. Patterson and R. H. Williams, ibid 17, 886 (1980).

16. W. A. Harrison, private communication.

17. R. W. Grant, J. R. Waldrop, S. P. Kowalczwk and E. A. Kraut, Phys. Rev., (in press).

18. W. Monch and H. Gant (to be published)

19. See Ref. 14 and ref. therein.

20. M. S. Daw and D. L. Smith, Phys. Rev. B20, 5150 (1979); Appl. Phys. Lett. 36, 690 (1980).

21. H. H. Wieder, Appl. Phys. Lett. 38, 170 (1981)

22. M. S. Daw and D. L. Smith, Solid State Comm. (to be published)

23. J. Lagowski, W. Walukiewicz, T. E. Kazior, H. C. Gatos and J. Siejka, in press, Sept.-Oct. (1980), J. Vac. Sci. Tech.; Jour. Appl. Phys.

24. To be published in the Sept.-Oct. issue of J. Vac. Sci. Tech.

25. Jour. Physical Soc. of Japan 49 (1980), Supp. A.

26. P. Skeath, C. Y. Su, I. Hino, I. Lindau, and W. E. Spicer, Appl. Phys. Lett. ~~in press~~ 39, 349 (1981).

27. G. P. Swartz, C. D. Thurmond, G. W. Kammlott, and B. Swartz, J. Vac. Sci. Tech. 17, 958 (1980).

28. W. E. Spicer, I. Lindau, P. Skeath, and C. Y. Su, J. Vac. Sci. Tech. 17, 1019 (1980).

29. P. W. Chye, C. Y. Su, I. Lindau, C. M. Garner, P. Pianetta, and W. E. Spicer, Sur. Sci. 88, 439 (1979).

30. G. Lucovsky and R. S. Bauer, J. Vac. Sci. Tech. 17, 946 (1980).

31. H. H. Wieder, J. Vac. Sci. Tech. 17, 1009 (1980).

32. L. G. Meiners, J. Vac. Sci. Tech., Sept-Oct. (1981), Issue in press.

33. D. Fritsche, Inst. of Phys. Conf. No. 50, pp. 258; ed. by G. G. Roberts and M. J. Morant, (The Institute of Physics, Bristol, 1980).

34. R. F. C. Farrow, A. G. Cullis, A. J. Grant, and J. F. Patterson, J. Crys. Growth, 45, 292 (1978).

FIGURE CAPTIONS

2 X The surface or interface energy defect levels obtained in this work. The energy of the levels are considered to be well established (within the experimental accuracy of ±0.1eV) as are the acceptor or donor nature of the levels. The identification in terms of missing anions or cations is less sure for GaAs and InP. For example, Harrison [ref. 16], Grant et al [ref. 17], and Monch et al [ref. 18] have suggested that both GaAs levels are due to the same defect and associated this with a missing As; In InP, Williams et al [ref. 15] associates the 1.2 eV donor with missing P and the 0.9 eV acceptor with missing In.

X Surface Fermi Level (E_{fs}) position versus logarythm of Au coverage. From the rise in E_{fs} for Au at low coverages in the p-type material, it is clear that the defect mechanism is working in that region. The drop in E_{fs} (above about $5x10^{14}/cm^2$ Au coverage) indicates the creation of a new interface level. This is believed to be due to a new state being created by the Au in the GaAs.

1(c)

1 X Surface Fermi level position (E_{fs}) in the energy gap of GaAs; (a) As a function of metal coverages for three different metals (Al, Ga, and In) deposited on both n- and p-type samples. (b) The stationary position of the Fermi level in the band gap after deposition of a fraction of a monolayer of oxygen and various metals. The value shown for Au at submonolayer coverage is considerably closer to the valance band maximum than the values of other metals or oxygen. (c) Changes with Au coverage from a small fraction of a monolayer up to ~10 monolayers on both n- and p-type samples.

UNIFIED MODEL FOR INTERFACE STATES AND SCHOTTKY BARRIERS

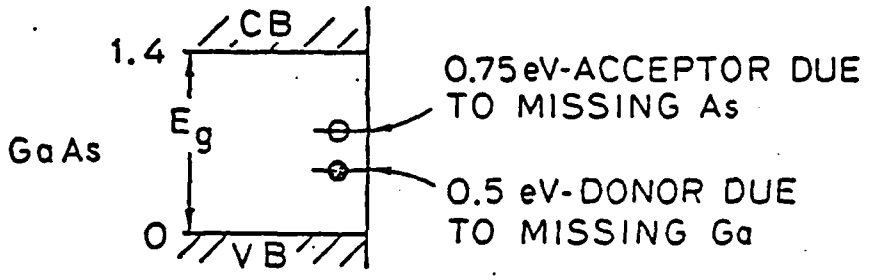

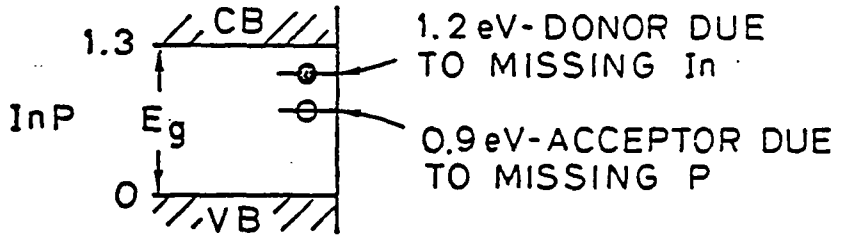

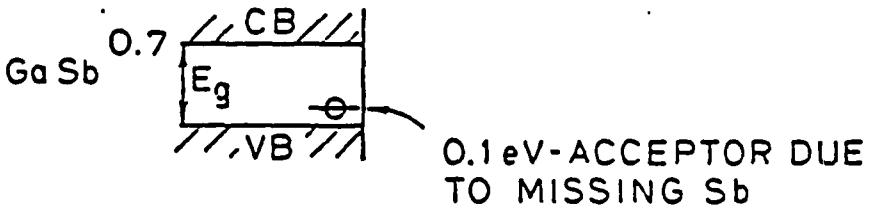

(new Fig. 1)

Fig. 2

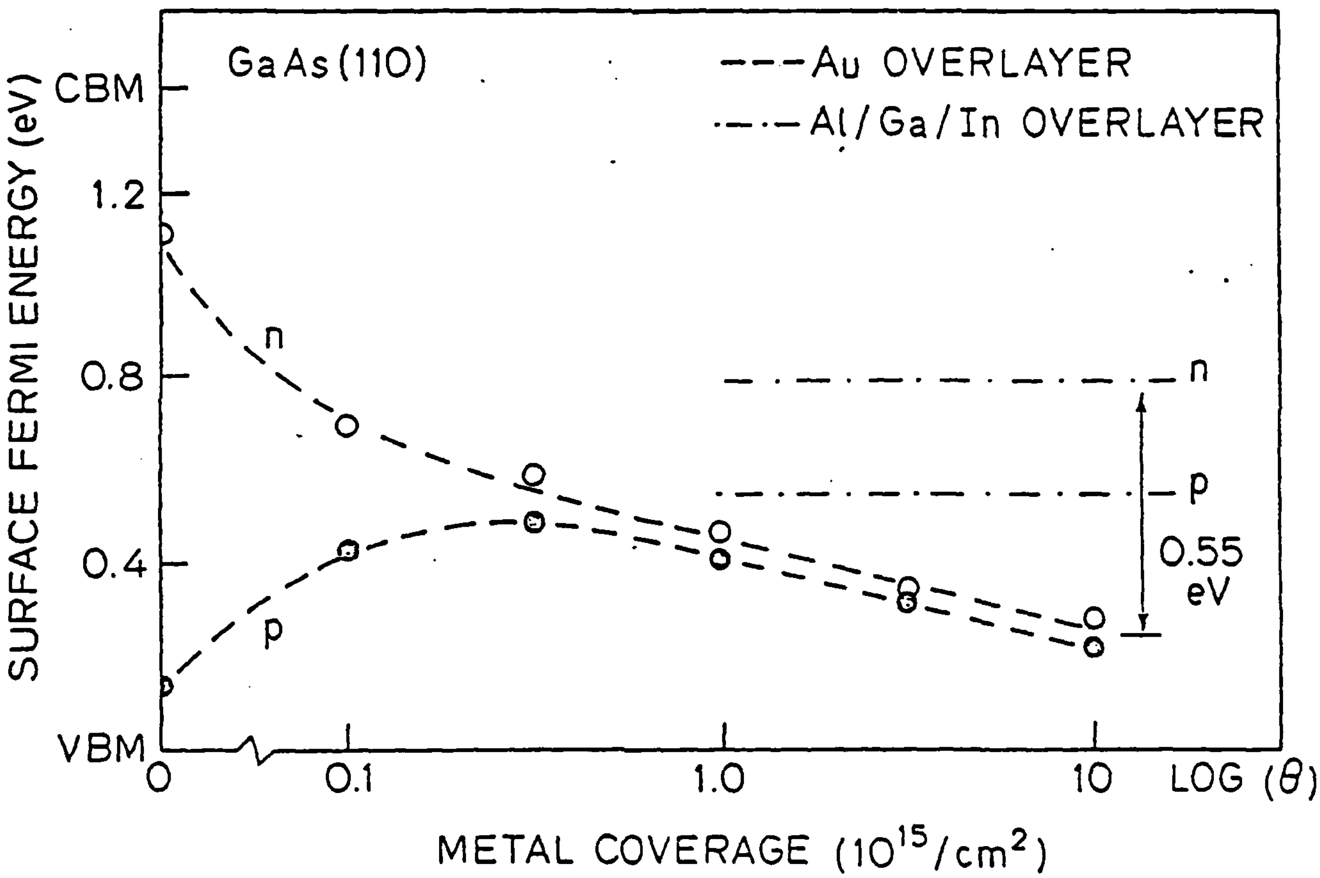

FIGURE 2

dilita.

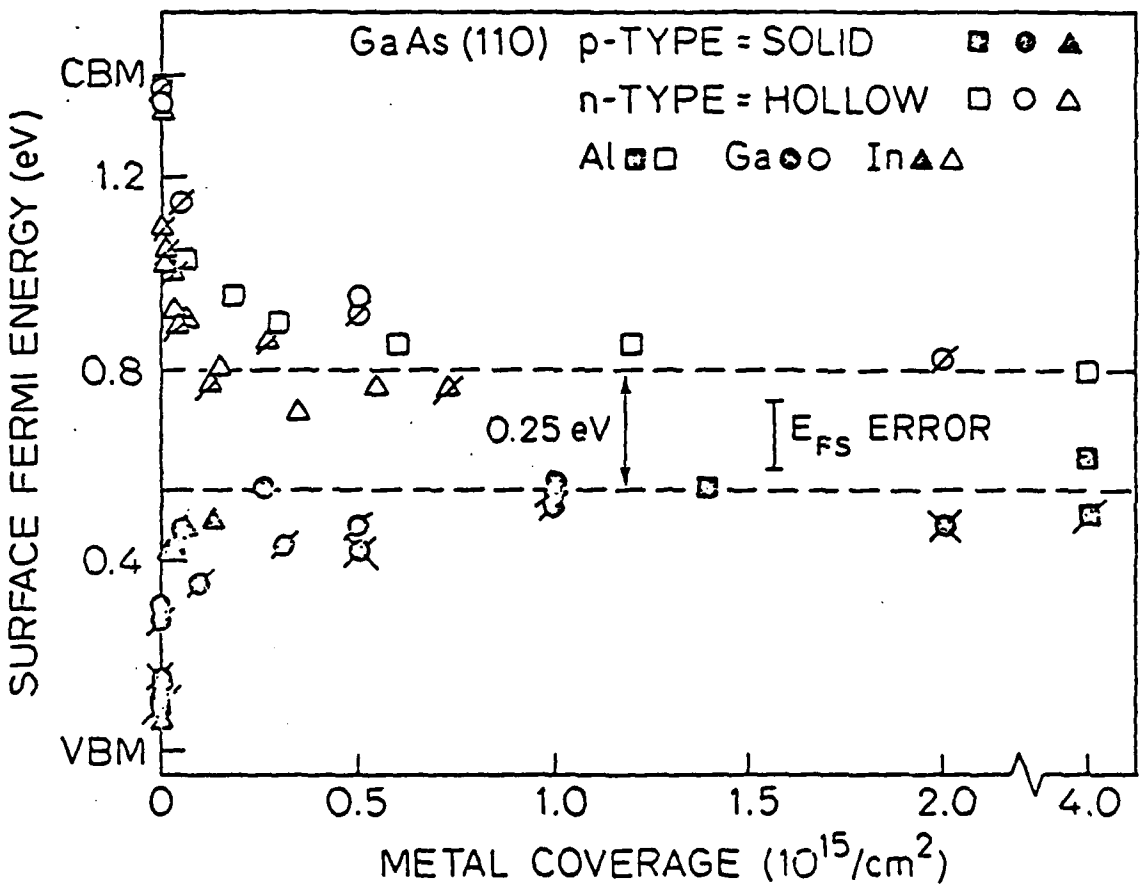

FIGURE 3

delete

APPENDIX H

Submitted to Chem. Phys. Lett.

PHOTOEMISSION STUDIES OF THE OXIDATION OF Cs+ --IDENTIFICATION OF THE MULTIPLET STRUCTURES OF OXYGEN SPECIES

Chung-Yi Su, I. Lindau and W. E. Spicer++
Department of Electrical Engineering
Stanford University
Stanford, CA 94305

ABSTRACT

Photoemission studies of the oxidation of Cs have been performed. Four different states of oxygen were observed to be sorbed into Cs; three of the four states have been definitively identified to be O^{-2}, O_2^{-2} and O_2^-. Little differential relaxation in the orbital energies is observed for O_2^{-2} sorbed in Cs, whereas significant differential relaxation is observed for O_2^-. The difference is attributed to the close-shell configuration of O_2^{-2} and the open-shell configuration of O_2^-.

+ Work supported by DARPA-ONR under Contract N00014-79-C-0072

++ Stanford W. Ascherman Professor of Engineering

The multiplet structure in the photoemission spectrum of free (gas phase) atom or molecule produced by photoionizing an incompletely filled atomic shell or molecular orbital has been the subject of many studies [1]. As has been pointed out by Rhodin and Broden [2], it is important to address the question whether the multiplet structure of a free atom or molecule can persist when that species enters a solid state environment (e.g., chemisorption): Delocalization of the electrons may reduce the coupling force giving rise to the multiplet structure, and the charge transfer accompanying the formation of chemical bonds may change the occupancy of the orbital under consideration and thus alter the multiplet structure. Successful interpretation of the change of the multiplet structure in going from free species to adsorbed species, is therefore of key importance to many chemisorption studies. One species of particular interest is oxygen. The multiplet structure of oxygen molecules physisorbed on metal surfaces became available recently [3]; attempts have been made thereafter to discuss the chemisorption of oxygen under other conditions in reference to the multiplet structure of physisorbed oxygen. There are, however, other oxygen species needed to be considered in even the simplest chemisorption system. In this paper, we report photoemission measurements of the adsorption of oxygen on thick Cs films at low temperature (~140° K). Cs has a 1.6 eV wide valence band which is separated by 10 eV from the next inner shell forming a wide band gap. Oxygen states thus fall in this band gap of Cs and have minimum intermixing with Cs states. Minimum intermixing of substrate-adsorbate states is also expected from the large electronegativity difference between Cs and O. Formation of ionic oxygen species, such as O^{-2}, O_2^{-2} and O_2^-, can be anticipated in oxidizing Cs. The O/Cs system thus

provides a unique opportunity for exploring the electronic structure of a series of ionic oxygen species. We will demonstrate the definitive identification of multiplet structures of O^{-2}, O_2^{-2} and O_2^-.

The experiments were carried out in a stainless-steel ultra-high-vacuum chamber with a base pressure of $\sim 7 \times 10^{-11}$ torr. Metallic Cs was evaporated onto clean substrates cooled to ~140° K to form thick (> 200 Å) Cs films. The light source used was synchrotron radiation from the Stanford Synchrotron Radiation Laboratory (SSRL). Energy analyses of photoelectrons were performed with a double-pass cylindrical-mirror-analyzer (Physical Electronics) and pulse counting electronics.

The discussion below will be divided into three parts. We will first present photoemission spectra of the different oxygen states that are identified. The spectra of these oxygen states are then compared to the multiplet structures of several free oxygen species. To complete the identification of the oxygen species formed in the oxidation of Cs, we will also compare the observed binding energies of various oxygen levels with the ionization energies of free ions.

The evolution of oxygen induced features in the valence band region with increasing oxygen exposure is complex. Previously, Wijers et al [4], showing difference curves only, have concluded the existence of only two different oxygen states. We have compared results from three different films with oxygen exposures ranging from 0.1 L to 200 L, at which point the oxidation process appears to have reached saturation and have identified four different states of oxygen. In Fig. 1, we display four specra which are selected such that in each spectrum features associated with one particular state of oxygen dominate. These states are labelled 1 through 4 in Fig. 1 in the order of their

appearance in the exposure sequence. Binding energies of the features of the four different states of oxygen in Cs are also summarized in Table 1.

A few explanations of Figure 1 and Table 1 are given below. Three features are actually observed for state 1 oxygen: one strong peak at 2.7 eV (labeled 1a in Figure 1) below Fermi level and two other weak features at 4.4 eV (1b) and 5.4 eV (1c). The two weak features with higher binding energies were previously interpreted as part of the multiplet structure for chemisorbed oxygen [2,4]. Here, by comparing with the plasmon features associated with Cs-5p core levels, they are found to be a surface plasmon (1.7 eV) and a bulk plasmon (2.7 eV) loss from the major oxygen peak at 2.7 eV BE side of the 5p levels. Hence, state 1 oxygen is characterized by a single peak in the photoemission spectrum. In the bottom curve of Fig. 1, some emission due to the three features of the state 2 oxygen can also be seen. The strongly rising emission overlapping with features 3c and 4e seen in Fig. 1 is due to the onset of Cs-5p levels.

We have also observed other spectroscopic changes accompanying the transition between different states of oxygen. For example, whenever the state 1 oxygen is observed (even with a significant amount of the state 2 oxygen mixed in), the surface remains metallic as evidenced by: (1) electron emission at the Fermi edge, (2) plasmon losses associated with the core levels, and (3) low yield for both the primary and the secondary photoelectrons when excited with 20-32 eV photon energies, which is a manifest of a short electron escape depth characteristic of the Cs metal. When the state 1 oxygen disappears completely, the surface becomes semiconducting

or insulating. More details of such changes will be given elsewhere.

In Fig. 2, we give the multiplet structure expected for ionizing, from top to bottom, O^{-2}, O_2^{-2} and O_2^-. Since only the energy separations will be compared, the leading peak is in all cases assigned as the energy zero. The relative height of the multiplets of an oxygen species indicated in Fig. 2 is simply the spin-orbit degaeneracy of the individual multiplets. The spin-orbit degeneracies are true measures of the relative intensity of these multiplets in a photoemission spectrum only if the ionization probabilities of all orbitals are equal.

In Fig. 2, we also indicated (with heavy short bars) the energy positions of the multiplets of three experimentally obsrved states: state 1 is compared to O^{-2}, state 2 is compared to O_2^{-2}, and state 4 is compared to O_2^-.

The O^{-2} ion has a close-shell configuration and gives a single peak (ignoring the very small spin-orbit splitting). This is the only oxygen species that give a single peak in the photoemission spectrum (neutral O atom gives three multiplets when ionized, as does O^-); hence, it is identified with state 1.

A few words should be said about the source of the multiplet structure for O_2^{-2} and O_2^- given in Fig. 2 before evaluating the comparisons with state 2 and state 4: (1) The multiplet splittings of the O_2^{-2} ion are taken from the MCSCF calculation of Krauss et al [6] with the O-O distance being 1.49 Å. The same values are also found in the compilation of combined theoretical-experimental data by Krupenie [7]. (2) the multiplet splittings of the O_2^- ion are taken from the compilation of Krupenie [7], whose results are in close agreement with the more recent GVB-CI calculation [8], with the O-O distance being

1.30 Å.

It is seen in Fig. 2 that an excellent agreement exists between the multiplet splittings of state 2 and the O_2^{-2} ion. The agreement between state 4 and the O_2^- ion is not as good, but a one-to-one correspondence for multiplets with binding energy lower than that of the $^3\Sigma_u^-$ multiplet is clear. The multiplets $^1\pi_g$, $^1\Delta_u$, and $^1\Sigma_u^+$, if present in the spectrum of the state 4 oxygen, are degenerate with the Cs-5p levels and are not observable. (A hint of the existence of these three multiplets in the spectrum has been observed as a reversal of the relative height of the two 5p peaks.)

The nearly perfect agreement between the multiplet splittings of free O_2^{-2} suggests that little differential relaxation has occurred for different molecular orbitals when inserting free O_2^{-2} ions into solid environment. This is expectd from the close-shell configuration of O_2^{-2}. Since all three molecular orbitals $3\sigma_g$. $1\pi_u$, and $1\pi_g$ are fully occupied, little interaction of these orbitals with the solid environment is expected. In contrast, significant differential relaxation in the orbital energies of the O_2^- ion is observed when inserting the free O_2^- ion into solids (the bottom panel of Fig. 2). This differential relaxation can be related to the open shell configuration of the O_2^- ion.

We now turn to the state 3 oxygen which has so far not been related to a particular oxygen species. Since state 3 appears at oxygen exposures intermediate to those required to produce state 2 (O_2^{-2}, related to Cs_2O_2) and state 4 (O_2^-, related to Cs_2O_4), one may anticipate it to be related to Cs_2O_3. In the work of Helms and Klemm [9], although the measured magnetic susceptibility can well be explained by two O_2^- one O_2^{-2} in the

$Cs_4(O_2)_3$ formulae-unit, the structural study has failed to show two types of geometrically inequivalent oxygen sites. O_2^- and O_2^{-2} ions are known to have significantly different sizes. Such difference in size, however, appears to be suppressed in the crystal lattic of Cs_2O_3, so that no special sites can be identified for either O_2^- or O_2^{-2}. It is not inconceivable that the oxygen species in Cs_2O_3 is also indistinguishable as far as the electronic structure is concerned and can be described by an average configuration of O_2^{-q}, where q has a nonintegral value between 1 and 2. Oxygen species with such an electronic structure may also account for the spectrum of state 3.

Overall, we have seen that the multiplet structures of oxygen adsorbed in the Cs films, with the exception of state 3, can be well understood in terms of the multiplet structures of free oxygen species.

Above we have compared the multiplet splittings, or the relative energy positions, of the adsorbed oxygen and the free ions. Below, we will attempt to predict the binding energies of the least bonded multiplet of state 1, 2, and 4 from the first ionization energies of O^{-2}, O_2^{-2}, and O_2^-.

The binding energy of an electron on an ion in a solid E_x is related to the free ion ionization energy E_{fi} through the equation

$$E_x = E_{fi} + E_b - E_r$$

where E_b is the additional binding energy introduced by the solid environment to the electron, and E_r is the extra atomic relaxation energy present in the photoemission process. To compare the calculated values with the measured binding energies referred to the Fermi level, E_x has to be corrected for the work function of the solid in question.

The following details also enter the calculation: (1) For Cs_6O and $Cs_{11}O_3$ clusters in Cs metal, the E_b contains an electrostatic term and the remoralization energy of the free electron gas in response to the negative changes localized on the O^{-2} ion; the latter term roughly cancels the work function term and the extra-atomic relaxation energy [10]. (2) For Cs_2O, there is a polarization term in E_b in addition to a Madelung term as suggested by Tsai et al [11]. This polarization term is about twice the extra atomic relaxation energy. The relaxation energy is calculated using a classical treatment of Jost [12]. The dielectric constant needed for the calculation is obtained from the experimental results of Heimann et al [13]. (3) For Cs_2O_2 and Cs_2O_4, E_b contains only Madelung contribution, and the Madelung energies were calculated using a semi-empirical equation developed by Broughton and Bagus [14]. The extra-atomic relaxation energies for these two compounds were also calculate with the electrostatic equation of Jost [12]. The dielectric constants needed were calculated using Lorentz-Lorenz formula [15]. (4) Values of the work function were extracted from the paper by Gregory et al [16].

The calculate values are compared to the experimental results in Table 2. The agreement is surprisingly good, considering all the approximations involved. The additional support rendered by Table 2 to the interpretations that state 1 being O^{-2}, state 2 being $\bar{2}^{-2}$, and state 4 being O_2^-, is gratifying.

In summary, we have observed four distinct oxygen species in the oxidation of thick Cs films at ~140°K. Three of the four species are definitively identified to be O^{-2}, O_2^{-2} and O_2^-. In each of these cases, a clear one-to-one correspondence between the multiplet structures

of the free species and the adsorbed species is found. Such persistance of the multiplet structure of the free species in a solid state environment is the resutl of a large ionicity difference between Cs and O, which assures a high degree of localization of the valence charges on the ionic oxygen species under consideration. The multiplet structure in the photoemission spectrum of O_2^{-2} in Cs is identical to that expected for free O_2^{-2}; no differential relaxation in orbital energies is observed. In contrast, significant differential relaxation in orbital energies is observed for O_2^- in Cs. This effect is attributed to the close-shell as opposed to open-shell, configuration of O_2^{-2}. The fourth state of oxygen was formed with oxygen exposures intermediate to those required to form O_2^{-2} and O_2^-, is suggested to be O_2^{-q} with $1<q<2$.

REFERENCES

1. J. W. Babalais, Principles of Ultraviolet Photo-electron Spectroscopy, Wiley, New York, 1977, Chaps. 4, 5.

2. T. N. Rhodin and B. Broden, Surf. Sci. 60, 466 (1976).

3. P. Hofmann, K. Horn, A. M. Bradshaw, and K. Jacobi, Surf. Sci. 82, L610 (1979); D. Schmeisser, K. Jacob; and P. M. Kolb, Proc. IVth Int. Conf. Solid Surfaces and IIIrd Cur. Conf. Surf. Sci.

4. C. Wijers, M. R. Adriaens, and B. Geuerbacher, Surf. Sci. 80, 317 (1979).

5. B. Feuerbacher, in Proc. 7th Intern. Conr. and 3rd Intern. Conf. Solid Surfaces, 1149 (Vienna, 1977).

6. M. Krauss, D. Neumann, A. C. Wahl, G. Das, and W. Zemke, Phys. Rev. A 7, 69 (1973).

7. P. H. Kruperne, J. Phys. Chem. Ref. Data 1, 423 (1972).

8. Moss and W. A. Goddard III, J. Chem. Phys. 63, 3523 (1975)

9. V. A. Helms and W. Klemm, Z. Anorg. Allg. Chem. 242, 201 (1939).

10. C. R. Helms and W. E. Spicer, Phys. Rev. Lett. 31, 1307 (1973).

11. K. -R. Tsai, P. M. Harris, and E. N. Lassettre, J. Phys. Chem. 60, 338 (1956).

12. W. Jost, J. Chem. Phys. 1, 466 (1933).

13. W. Heimann, E. -L. Hoene, S. Jeric, and E. Kansky, Exp. Tech. Phys. 21, 193-207, 325-341,431-436 (1973).

14. J. Q. Broughton and P. S. Bagus, J. Electron. Spectr. Related Phenomena 20, 261 (1980).

15. N. F. Mott and R. W. Gurney, Electronic Processes in Ionic Crystals, 2nd ed., Chap. 2, pp. 18, Dover, New York, 1964.

16. P. E. Gregor, P. Chye, H. Sunami, and W. E. Spicer, J. Appl. Phys. 46, 3525 (1975).

Table 1

SUMMARY OF BINDING ENERGIES OF THE MULTIPLETS OF DIFFERENT OXYGEN STATES OBSERVED IN THE OXIDATION OF Cs

State Label	Binding Energies (eV below Fermi level)
1	2.7, (4.4), (5.4)
2	3.3, 6.4, 7.8
3	5.5, 8.3, 10.4
4	4.7, 5.8, 8.5, 10.7

Table 2

COMPARISON OF CALCULATED AND MEASURED BINDING ENERGIES OF OXYGEN LEVELS OF VARIOUS OXYGEN SPECIES

Compound or Cluster	Cs_6O in Cs	$Cs_{11}O_3$ in Cs	Cs_2O	Cs_2O_4	Cs_2O_4
Oxygen Species	O^{-2}	O^{-2}	O^{-2}	O_2^{-2}	O_2^-
E_{fi} (eV)	-6.5	-6.5	-6.5	-1.6	0.56
E_{fx} (eV) (calculated)	3.66	2.45	2.64	3.20	4.85
E_{exp} (eV)	2.7	2.7	2.7	3.3	4.7

Figure Captions

1. Photoemission spectra of four different states of oxygen in Cs. Spectra were taken with 30 eV photon energy. Each spectrum is dominated with features from one state of oxygen and those features are marked with vertical bars. Oxygen exposures required to produce the various states of oxygen increases from bottom to top.
2. Comparison of the multiplet structures of free ions and of oxygen adsorbed in Cs: O^{-2} with state 1 (top), O_2^{-2} with state 2 (center), and O_2^- with state 4 (bottom). The short bars at the top of each panel indicate the relative energy positions of the photoemission features shown in Fig. 1. Only energy separations are compared; in all cases, the energy zero is chosen to be the energy position of the leading oxygen multiplet. Designations of the multiplets are indicated on top of each thin vertical bar, and the molecular orbital origins of each multiplet are also indicated below the bars.

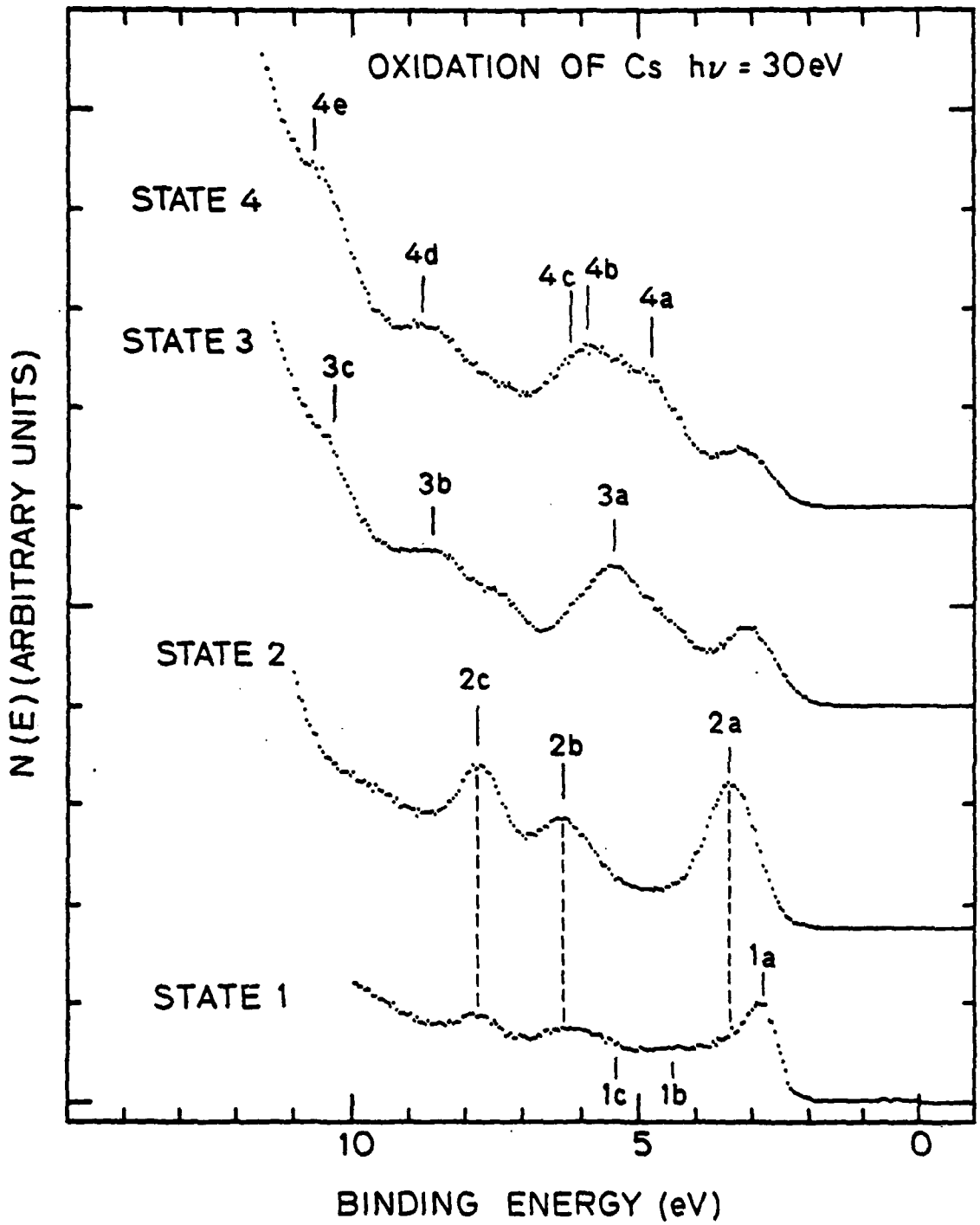
OXIDATION OF Cs hν = 30eV
4e
STATE 4
4d
4c
4b
4a
STATE 3
3c
3b
3a
STATE 2
2c
2b
2a
STATE 1
1a
1c
1b
N(E) (ARBITRARY UNITS)
10
5
0
BINDING ENERGY (eV)

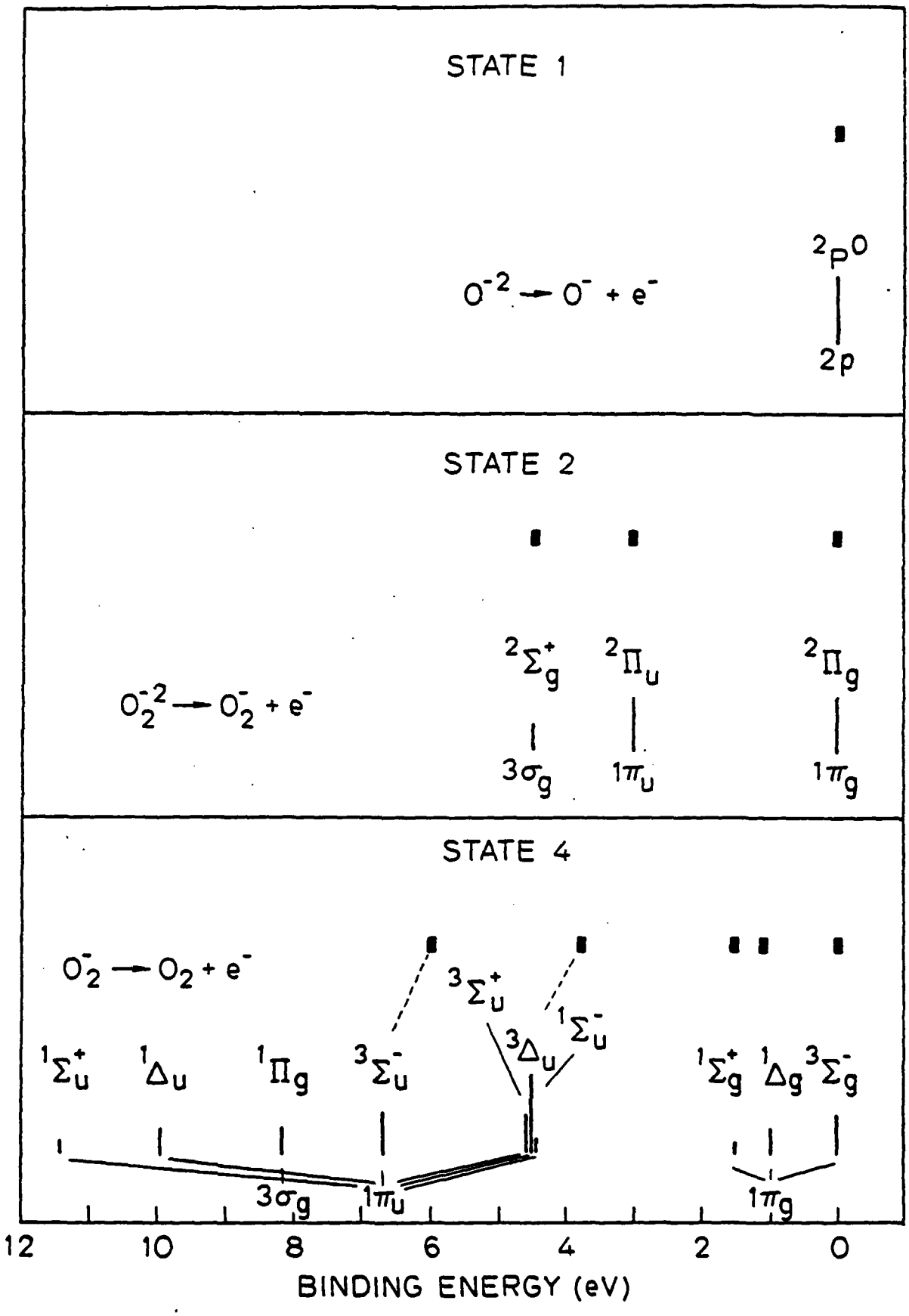
STATE 1
$O^{-2} \rightarrow O^- + e^-$
$^2P^O$
2p
STATE 2
$O_2^{-2} \rightarrow O_2^- + e^-$
$^2\Sigma_g^+$
$^2\Pi_u$
$^2\Pi_g$
$3\sigma_g$
$1\pi_u$
$1\pi_g$
STATE 4
$O_2^- \rightarrow O_2 + e^-$
$^3\Sigma_u^+$
$^1\Sigma_u^-$
$^1\Sigma_u^+$
$^1\Delta_u$
$^1\Pi_g$
$^3\Sigma_u^-$
$^3\Delta_u$
$^1\Sigma_g^+$
$^1\Delta_g$
$^3\Sigma_g^-$
$3\sigma_g$
$1\pi_u$
$1\pi_g$
12
10
8
6
4
2
0
BINDING ENERGY (eV)


DAT
ILM